JPRS: 16,269

20 November 1962

OT

18

SOVIET STUDIES IN POWDER METALLURGY

U. S. DEPARTMENT OF COMMERCE
OFFICE OF TECHNICAL SERVICES
JOINT PUBLICATIONS RESEARCH SERVICE
Building T-30
Ohio Dr. and Independence Ave., S.W.
Washington 25, D. C.

Price: $5.60

658 500

FOREWORD

This publication was prepared under contract for the Joint Publications Research Service, an organization established to service the translation and foreign-language research needs of the various federal government departments.

The contents of this material in no way represent the policies, views, or attitudes of the U. S. Government, or of the parties to any distribution arrangements.

PROCUREMENT OF JPRS REPORTS

All JPRS reports are listed in Monthly Catalog of U. S. Government Publications, available for $4.50 ($6.00 foreign) per year (including an annual index) from the Superintendent of Documents, U. S. Government Printing Office, Washington 25, D.C.

Scientific and technical reports may be obtained from: Sales and Distribution Section, Office of Technical Services, Washington 25, D. C. These reports and their prices are listed in the Office of Technical Services semimonthly publication, Technical Translations, available at $12.00 per year from the Superintendent of Documents, U.S. Government Printing Office, Washington 25, D. C.

Photocopies of any JPRS report are available (price upon request) from: Photoduplication Service, Library of Congress, Washington 25, D. C.

SOVIET STUDIES IN POWDER METALLURGY

[Following is the translation of several articles in the Russian-language book Issledovaniya po Zharoprochnym Splavam (Research on Refractory Alloys), Vol 8, USSR Academy of Sciences Press, Moscow, 1962. Additional bibliographic information accompanies each article.]

TABLE OF CONTENTS

THE EFFECT OF ALLOYING ON THE STRUCTURE AND PROPERTIES OF POWDER-METAL HARD ALLOYS OF TUNGSTEN CARBIDE AND COBALT

[Following is the translation of an article by V. F. Funke, V. I. Tumanov, Z. S. Trukhanova in the Russian-language book Issledovaniya po Zharoprochnym Splavam (Research on Refractory Alloys), Vol 8, USSR Academy of Sciences Press, Moscow, 1962, pp 88-95.]

The carbides of the high melting point metals of the IV-VI groups of the periodic system belong to the class of metal-like compounds which are characterized by extreme hardness and temperature resistance (Ref 1).

At present carbide base alloys have been developed and widely applied in which high toughness and strength have been attained by the introduction of relatively small quantities of the plastic metals, Co and Ni. The metalloceramic heat-resistant alloys based on titanium carbide (Ref 2) and the hard alloys TiC-WC-Co (Ref 3) have been most widely applied in practice. The properties of the metalloceramic hard alloys are dependent on the composition and the pattern of the distribution of the bonding phase among the carbide grains and this is to a large extent determined by the wetting of the carbide base by the cobalt and nickel.

This paper presents the results of an investigation of the effects of the composition of the alloys of the WC-Co system.

The determination of the wetting edge angle by the method of quiescent drops showed (Table 1) that cobalt and nickel completely wet tungsten carbide, i.e. the edge angle (θ) is equal to zero for the WC-Co and WC-Ni systems. With an increase in the titanium carbide content in the carbide phase the edge angle increased to 21° in an alloy containing 23.6% TiC and to 38° in the TiC-Ni system.

Table 1

Wetting edge angles of nickel in the system WC-Ti, C-Ni

(a) Состав карбида, %		(b) Краевой угол θ
WC	TiC	
100	0	0°
100	0	0
76.4	23,6	21
0	100	38

(c) • Для кобальта.

(a) carbide composition, %
(b) edge angle
(c) for cobalt

In alloys of the system WC-Co the carbide grains are enveloped in a continuous film of cobalt (Ref 4) even at very small content (about 1%) of the binding metal while in the TiC-Co alloys they form conglomerates. In the two-phase alloys consisting of a solid solution of WC in TiC and a cobalt phase there is a continuous bond between the grains of the carbide (Ref 5). When the WC content is 70% and above the alloys consist of three phases: structurally free tungsten carbide, a solid solution of WC in TiC, and a cobalt phase. With an increase on the content of structurally free tungsten carbide to 40-50% by volume (15-20% TiC) the continuous bond between the carbide grains is destroyed, although the conglomerates of the grains of the titanium phase in which the WC phase is included (Ref 6) are maintained.

Fig 1 presents the variation of the ultimate strength in bending and the hardness of the alloys of the system TiC-WC-Co as a function of the content of titanium carbide in the carbide phase for a series of alloys with the same percent of cobalt by volume (7 and 25%). The WC-Co alloys have the highest strength. With an increase in the titanium carbide content to 30% the strength falls to a magnitude of about 80 kg/mm^2 and then stays constant as the titanium carbide content is further increased (curve 2). An increase in the cobalt content to 25% by volume (curve 3) is accompanied by a significant rise in strength (by about 80 kg/mm^2) in alloys with 5 and 15% TiC and a rather small rise in the alloys containing 30% or more TiC. The different influence of an increase in the cobalt content on the properties of alloys which differ only in the titanium carbide content can be explained by either essential differences in the composition of the solid solution on the cobalt base or a different pattern of the cobalt distribution. Although the composition of the cobalt phase may change, these changes in the alloys containing 5, 15, and 30% TiC cannot be significant since all these alloys are located within the boundaries of the three-phase domain of the phase diagram TiC-WC-Co (phases: TiC, WC, and cobalt). Alloys with a high TiC content lie within the boundaries of the two-phase domain. The sharpest changes in the properties might be expected not within the boundaries of the three and four-phase domain but at the transition to the two-phase, i.e. in the area from 30 to 60% TiC. The noted differences in the pattern of the structure of the alloys also affects the character of their fracture. It is known (Ref 7) that the weakest point in the WC-Co alloys is at the WC-Co boundaries and stress cracks appear on the boundary of separation of the WC phase and the cobalt. In the

TiC base alloys the cracks originate and propagate along the grains and conglomerates of the titanium phase which are formed as a result of incomplete wetting (Ref 8).

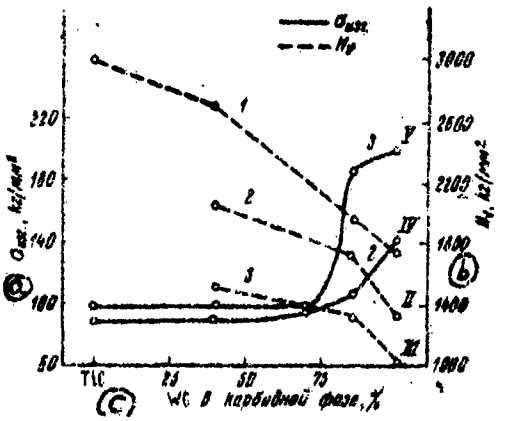

Fig 1. Variation of the ultimate bending strength and hardness of alloys of the system TiC-WC-Co as a function of the carbide phase composition:
1 - alloys containg no cobalt
2 - alloys with 7% Co by volume
3 - alloys with 20% Co by volume
(a) ultimate bending strenth, kg/mm^2
(b) hardness, Hv, kg/mm^2
(c) % WC in carbide phase

In WC-Co alloys with low Co content the thin layers of cobalt are "blocked" by the faces of the carbide grains and cannot undergo plastic deformation (Ref 9). Increasing plasticity by means of increasing the cobalt content leads to relaxation of the stresses which in conditions of brittle fracture provides increased strength of the alloys. In the absence of continuous bonds between the grains of carbide, increasing the cobalt content will lead to a sharp rise in the strength.

In alloys containing 30% or more TiC the carbide phase becomes the determing factor and increasing the cobalt content has little effect on the strength of the alloys in which continuous bonds between the carbide grains are present.

The hardness of the alloys TiC-WC-Co which consist of hard and brittle carbide phases and a cobalt-base plastic phase is determined by the composition of the carbide phase and the cobalt content. The hardest alloys are those which contain no cobalt (Fig 1, curve 1). Pure tungsten carbide of stoichiometric composition has a hardness of 1750 kg/mm^2 and the hardness increases with an

increase in the titanium carbide content. The introduction of cobalt reduces the hardness, however the pattern of its variation as a function of the titanium carbide content in the TiC-WC-Co alloys is analagous to that in the TiC-WC alloys.

The data on the variation of the bending ultimate strength and hardness for the alloys studied as a function of the cobalt content are presented in Fig 2. The curve showing the variation of the bending ultimate strength for two-phase alloys WC-Co passes through a maximum (curve 1). In the case of the three-phase alloys TiC-WC-Co in which the TiC content was 50% by volume or 15% by weight, X-ray structural studies (Ref 6) showed that the titanium phase was under tensile stress arising as a result of the difference in the coefficients of thermal expansion of the titanium phase and of the WC phase which it surrounds.

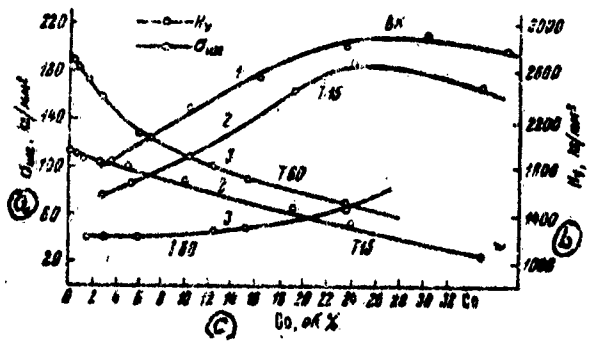

Fig 2. Effect of cobalt concentration on the bending ultimate strength and hardness H_V of the TiC-WC-Co alloys:
1 - WC-Co, 2 - WC-TiC-Co (15%TiC in carbide),
3 - WC-TiC-Co (6%TiC in carbide)
(a) bending ultimate strenth, kg/mm^2
(b) H_V, kg/mm^2
(c) % by volume of Co

Fig 2 shows that the shape of the curve for the variation of the bending ultimate strength as a function of the cobalt content for the WC-TiC-Co three-phase alloys (curve 2) is analagous to the shape for the WC-Co alloys. The strength curve passes through a maximum. This similarity, in spite of the considerable difference in the structure of the alloys, is explained by the fact that in both cases the increase in the cobalt content leads to an increase in the plasticity, is accompanied by a relaxation of the stresses, and increases the strength of the alloy. The difference lies in the circumstance that the fracturing stresses arise

in the WC-Co alloys in the cobalt levers while in the TiC-WC-Co alloys they arise in the carbide phase. The causes of the lowered strength of the low-cobalt WC-Co and TiC-WC-Co alloys are different: in the WC-Co alloys (curve 1) almost complete retardation of the plasticity of the cobalt layers takes place as a result of binding by the grains of the WC phase, while in the TiC-WC-Co alloys (curve 2) stresses arise in the carbide phase as a result of the different coefficients of thermal expansion of the WC and the TiC phases.

In the TiC-WC-Co two-phase alloys which consist of the TiC phase and a cobalt-base solid solution, the low ultimate tensile strength in the carbide are practically non-existent and an increase in the cobalt content does not lead to an increase in plasticity as long as the continuous carbide "skeleton" is maintained (curve 3). The hardness of these alloys changes very little up to 15% by weight of cobalt (20% by weight). Further increase in the cobalt content leads to fracture of the carbide "skeleton" and is accompanied by an increase in strength.

The hardness of the TiC-WC-Co alloys, both two- and three-phase, decreases almost linearly with an increase in the cobalt content (Fig. 9) and practically does not depend on the heat treatment or the composition of the cementing phase.

In alloys where a continuous bond between the carbide grains is absent, a change in the composition of the binding phase as a whole has a decisive effect on the properties of the alloy (Figs. 10, 11). On introduction of an alloying additive into the binding phase, which during the sintering process is found in a molten state, the penetration of the alloying component into the carbide phase is limited by the rate of diffusion into the hard carbide. As a rule the volume occupied by the binding phase is far smaller than the carbide phase volume so that a relatively small quantity of the alloying element can significantly influence the properties of both the binding phase and the entire alloy as a whole without a noticeable change in the composition of the carbide phase.

In this investigation we studied the effect of small quantities of Zr, V, Mo, Cr, and W on the structure and the properties of the tungsten carbide-cobalt alloys. The alloying components were introduced into the mixture during milling. The sintered alloys were subjected to X-ray structural analysis and separate chemical analysis of the cementing and carbide phases. The bending ultimate strength and the Vickers hardness were determined at temperatures of 20, 600, and 800°C.

The data from the X-ray structural analysis of the alloys and the distribution of the alloving additives are presented in Table 2.

Table 2

Chemical composition and X-ray structural analysis of the binding and carbide phases of WC-Co alloys

(a)	(b)	(c)	(d) (e) W (f)	(d) (e) W (g)	(d) (e) (f)	(d) (e) (g)	(h) (f)	(h) (g)	(h) (l)	(i) (j) a	(i) (j) c	(k)
[illegible]	15,0	...	1,28	0,3[illegible]	—	—	—	-		2,901[illegible]	2,830[illegible]	[illegible],547
Cu	[illegible],56	1,83	—	—	17,[illegible]	16,6	—	—	—	2,900[illegible]	2,831[illegible]	3,548
Mo	9,0	11,1	2,[illegible]	0,60	4,6	3,08	11,7	21,4	95,5	2,9008	2,8506	3,561
Cr	11,38	2,06	1,05	0,60	6,[illegible]	7,2	1,47	5,3	62,0	2,9010	2,820[illegible]	[illegible],559
Al	11,54	2,31	--	—	8,5	15,2	16,8	10,6	57,0	2,8997	2,8297	3,554
Cr, B Cr	14,72	2,43	0,4	0,10	14,0	15,5	0,04	0,16	1,5	2,8980	2,8320	3,557
B		4,42			7,6	30,1	3,97	42,0	74,0			

(m) Рентгеноструктурные исследования проведены А. Е. Ковальским и Л. Х. Пивоваровым.

(a) alloying component
(b) cobalt content, % by weight
(c) alloying component content, % by weight
(d) composition of the cementing phase, %
(e) WC alloying component
(f) weight %
(g) atomic %
(h) alloying component content in carbide phase
(i) lattice parameters
(j) WC phase
(k) cobalt base solid solution
(l) % total content in alloy
(m) X-ray structural analysis performed by A.E. Koval'skiy and L.Kh. Pivovarov

The data of Table 2 show that in the alloys containing copper and aluminum the cobalt phase does not contain tungsten carbide in solution. In the WC-Co alloy without alloying additives the cobalt phase contains more then 1% WC.

Copper and aluminum are soluble in cobalt in rather large quantities (Refs 12, 13). However, these components differ significantly in the character of their interaction

with the carbide phase. The copper does not react with tungsten carbide while 57% of the Al transforms into the carbide phase, accompanied by a considerable reduction in the parameters of the tungsten carbide lattice. Molybdenum and chromium are distributed between the carbide and cementing phases which also contain tungsten carbide in solution.

The concentration of the cobalt based solid solution during alloying with the carbide-forming elements (Mo, Cr, Al) increases with an increase in the free energy of formation of their carbides but the percentage of the alloying metal transformed to the carbide phase is decreased.

The introduction of boron in the form of chromium boride into an alloy containing chromium leads to a significant change in the distribution of the chromium between the phases. The concentration of chromium in the solid solution rises while its content in the carbide phase becomes very low. The majority of the boron (74%) is transformed into the carbide phase although its content in the cobalt phase remains high (7.6%).

These data show that the action of the alloying components differs considerably and this has an influence on the properties of the alloys (Fig 3, 4).

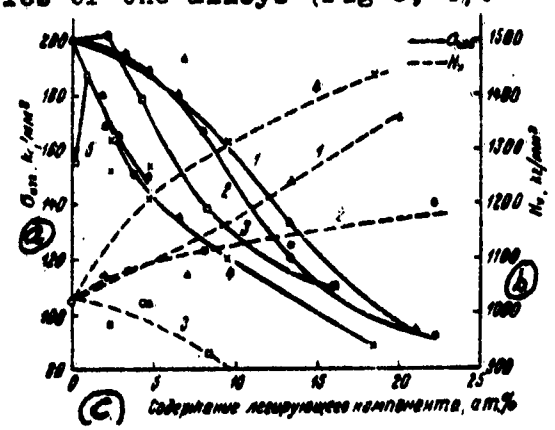

Fig 3. Effect of the content of an alloying component (to the binding metal) on the bending ultimate strength and the hardness of WC-Co alloys at a temperature of 20°:
1 - molybdenum (15% Co), 2 - chromium (15% Co), 3 - aluminum (15% Co), 4 - chromium boride (15% Co), 5 - copper (6% Co)
a bending ultimate strength, kg/mm^2
b H_V, kg/mm^2
c content of the alloying component, atomic %

At room temperature all the alloying components studied, with the exception of copper, lowered the bending ultimate strength of the WC-Co alloys. The greatest lowering of the strength is noted when alloying with chromium boride, somewhat less with aluminum, still less with chromium, and the least with molybdenum. The concentration of the alloying components in the solid solution of the cobalt base decreases in the same order (Table 2).

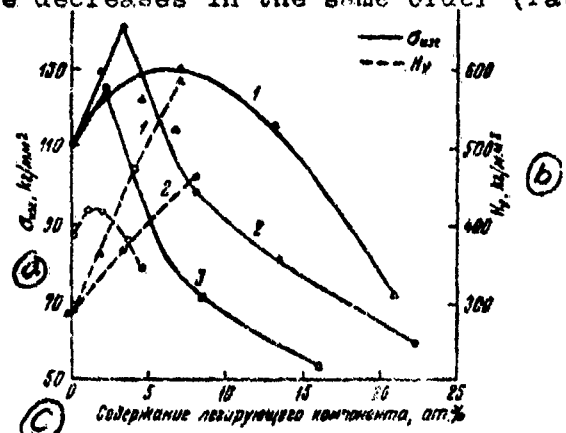

Fig 4. Effect of content of alloying component (to binding metal) on the bending ultimate strength and hardness of the WC-Co alloys at elevated temperatures:
1 - molybdenum (800°), 2 - chromium (800°)
3 - aluminum (800°), 4 - copper (600°)
(a) bending, ultimate, kg/mm^2
(b) hardness, kg/mm^2
(c) alloying component content, atomic %

The introduction of small quantities of copper (to 1%) leads to an increase in the strength of the alloys while a further increase in copper content is accompanied by a decrease in the strength of the WC-Co alloys. Alloying with chromium boride, aluminum, chromium and molybdenum increases the concentration of the alloying components (W, Cr, Al, Mo) in the cobalt-base solid solution, decreases the plasticity, and leads to a reduction in the strength of the alloys. The greater the concentration, the larger the reduction in strength. The composition of the binding phase has little effect on the hardness of the alloys since the hardness varies nearly linearly with the change in the cobalt content while the volumetric content of the binding phase in the alloys studied did not exceed 20%. The maximum increase in hardness was observed when alloying

with chromium boride, less in the case of molybdenum, and least when alloying with chromium. Alloying with aluminum is an exception, and this is probably related to the reduction of the hardness of the carbide phase.

At elevated temperatures (600°, 800°), alloying with Mo, Cr, Al and CrB_2 is accompanied by a significant increase in the strength of the alloys (Fig 4) since in these cases the lowering of the plasticity of the cementing phase becomes a favorable factor. However, the maximum on the strength--content-of-alloying-component curve is different for each of the alloying additives. The higher the content of the alloying additive in the cobalt-base solid solution (Table 3), the lower the concentration of the alloying component in the alloy at which the maximum strength is observed. This corresponds to that content of the alloying additive for which further strengthening of the cobalt by alloying so reduces its plasticity that even at the test temperature of 800° the alloy strength is reduced.

The increase in the hardness of the alloys at the 800° temperature (with alloying) is far larger than at room temperature (Fig 4). The increase in hardness when using molybdenum as an additive is considerably more than when using chromium, and this is probably determined by the larger atomic concentration of the molybdenum in the carbide phase.

The effect of the additions on the properties of the alloys is determined not only by the concentration of the solid solution but also to a considerable extent is dependent on the nature of the additive component. It is known (Ref 14) that W, Mo, Cr, and Al lead to a sharp strengthening of the Ni and Co alloys at room temperatures and at elevated temperatures. Copper is not used as an additive component to strengthen the nickel and cobalt alloys.

Table 5 presents the data on the effect on the properties of the WC-Co alloys of additions of copper. As can be seen from the table, the introduction of 20% copper to the binding phase reduces the strength and hardness of these alloys.

With a copper content up to 1-2 atomic % the plasticity of the cementing phase increases as a result of the absence of dissolved tungsten carbide and this leads to an increase in strength.

At 600° the increase in strength is already practically nonexistent while the strengthening action of the other additive components (Mo, Cr, Al) is most appreciable at the elevated temperatures.

Table 3

Effect of copper (20 % by weight to cobalt) on the properties of the WC-Co alloy

Содержание меди, вес. % (a)	Содержание кобальта, вес. % (b)	$\sigma_{изг}$, кг/мм² (c)		H, кг/мм² (d)
		20°	500°	
20	8	144	117	878
—	8	188	177	1103
20	15	152	142	896
—	15	231	177	928
20	30	137	108	558
—	30	165	142	578

(a) copper content, weight %
(b) cobalt content, weight %
(c) ultimate bending strength, kg/mm²
(d) H, kg/mm²

The properties of the powder metal hard alloys WC-Co may be substantially improved by the selection of additive components, the choice of which to a considerable extent must be determined by the pattern of their interaction with the cementing and carbide phases.

The carbide base powder metal hard alloys consist of hard, but brittle carbide grains and plastic constituents (WC, Co, Ni). The carbides are characterized by high strength and hardness at elevated temperatures while iron, cobalt, and nickel are outstanding for their relatively slight weakening at high temperatures. The cementing metals are introduced in the minimum quantities sufficient to attain the necessary toughness of the alloys.

It is clear from the data obtained in this investigation that in those alloys in which there is a continuous bond between the carbide particles, an increase of the cobalt content reduces the hardness of the alloys and does not lead to a significant improvement in their strength (alloys WC-Co and TiC-Wc-Co with TiC content up to 20-30%). In the systems in which there is not a strong continuous bond between the grains of the carbide phase, the introduction of a cementing metal in the same volumetric proportions as used in the previous case leads to a considerable increase in strength (alloys C-Co and TiC and C-Co with TiC content up to 20-30%).

The structure of the alloys, the existence or absence of continuous bonds between the carbide particles, is primarily determined by the capability of the cementing

metal to wet the carbide. In order to alloy the carbide phase it is necessary to have components which, while increasing the hardness and the thermal resistance of the carbide base, can also improve the wetting of the carbide by the binding metal. The optimum case is a system in which complete wetting of the carbide by the cementing metal is achieved, i.e. there is not continuous bond between the grains of the carbide base. In such a system further improvement of the properties is possible by changing the composition and properties of the cementing phase.

The experiments conducted indicated that when alloying the cementing phase the alloying components can be divided into two groups: the first group consists of those elements which on introduction reduce the solubility of the tungsten carbide in the cobalt (in our case these were copper and aluminum), and the second group consists of those elements which increase the thermal resistance of the cement and of the alloy as a whole (in our case Mo, Cr, Al) as a result of the increased concentration of the alloying components. The elements of the first group should be added in very small quantities, just sufficient to prevent the solution of the carbide in the binding metal. In this case there is an increase in the plasticity of the cementing metal and an increase in the strength of the alloy as a whole. Increasing the quantity of the alloying component and consequently increasing its concentration in the solid solution reduced the properties of the alloy. The optimum content of the alloying components of the second group is determined by their distribution between the cementing and the carbide phases, by their strengthening action on the cementing metal, and also by the operating temperatures of the given material. The composition of the cementing phase should be such that there is a minimum reduction of strength and plasticity of the alloys at room temperature while the maximum possible increase in strength at operating temperature is attained.

CONCLUSIONS

1. The relation between the composition of the carbide phase and the structure and the properties of the alloys of the system WC-TiC-Co is shown.

2. The dependence of the properties of the alloys WC-Co and WC-TiC-Co (two and three-phase) on the cobalt content is presented.

3. Data were obtained on the distribution of the additive components (Cu, Mo, Cr, Al, CrB) between the cementing and carbide phases in the WC-Co alloys.

ON THE STRUCTURE OF ALLOYS OF TITANIUM CARBIDE WITH NICKEL, CHROMIUM, AND MOLYBDENUM

[Following is the translation of an article by V. N. Yeremenko, Z. I. Tolmacheva, and T. Ya. Velikhanova in the Russian-language book Issledovaniya po Zharoprochnym Splavam (Research on Refractory Alloys) Vol 8, USSR Academy of Sciences Press, Moscow, 1962, pp 95-102.]

In the development of the hard and abrasion-resistant alloys and the refractory materials with a titanium carbide base and using metallic binders such as nickel, chromium, and molybdenum it is important to have accurate data on the interactions of titanium carbide with these metals and on the structure of the alloys of titanium carbide with nickel, chromium, and molybdenum. The information available in the literature on this subject is based on the experimental data of various investigators and is neither consistent nor reliable. In the majority of the publications it is indicated that the interaction of titanium carbide with these metals results in the formation of either the carbides of these metals (Refs 1, 2) or the release of free carbon (Ref 3). These conclusions contradict the conclusions which may be drawn concerning the progress of the reactions in the systems TiC-Me (Me standing for nickel, chromium, or molybdenum) on the basis of the thermodynamic stability of the carbides of the metals of these elements.

The bonding of the cementing metal into the brittle carbides should significantly alter the properties of the materials consisting of a titanium carbide base and a metallic binder. First of all, this should lead to an increase of the already high brittleness of the titanium carbide base alloys. The release of free graphite in the alloys is also undesirable since this results in a lowering of the mechanical strength.

The present work on the triangulation of the systems Ti-C-Ni, Ti-C-Cr, and Ti-C-Mo was undertaken in order to clarify the actual phase composition of the alloys of titanium carbide with nickel, chromium, and molybdenum.

THE TITANIUM-CARBON-NICKEL SYSTEM

A summary of the available data on the Ti-C and Ti-Ni systems is given in Ref 4, that on the Ni-C system in Ref 5 and the interaction of titanium carbide with nickel is discussed in Refs 6, 7, 18.

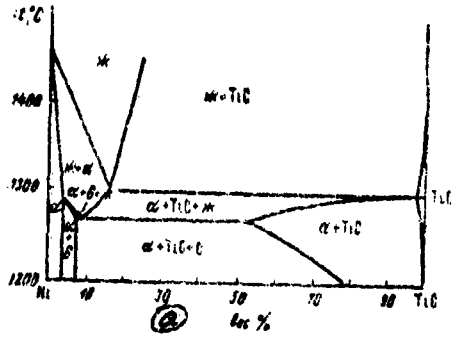

Fig 1. Phase fields in alloys of titanium carbide with nickel (Refs 3, 9)

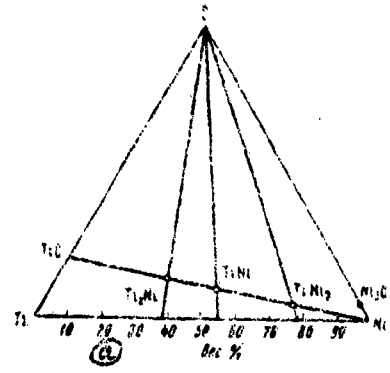

Fig 2. Composition of the alloys studied

(a) % by weight

There are varied ideas on the structure of the alloys of titanium carbide with nickel. According to the diagram published by Steinitz (Ref 9) with references to Stev's work and according to the later publication of Ref 3 (Fig 1), there is an extensive three-phase field in the TiC-Ni section of the ternary system Ti-C-Ni, formed by titanium carbide, graphite, and a nickel-base solid solution. On this basis the conclusion was drawn that the TiC-Ni section is not quasibinary. On the other hand, investigations reported in Refs 10 and 8 gave a basis for concluding that the TiC-Ni section is quasibinary and has a phase diagram of a simple eutectic type similar to the situation existing in the TiC-Co (Refs 12, 13) and TiC-Fe (Ref 14) systems.

Since in the system Ti-Ni there are three compounds, --Ti_2Ni, TiNi, and $TiNi_3$--, the nickel carbide Ni_3C is not stable at temperatures below 2000° (Ref 5), and the free energy of formation from the elements is positive up to 3500° (Ref 11), in order to arrive at a final conclusion concerning the character of the section TiC-Ni of the ternary system Ti-C-Ni an investigation was made of the structure of alloys whose composition lies at the points of intersection of the TiC-Ni sections with the sections Ti_2Ni-C, TiNi-C, and $TiNi_3$-C (Fig 2).

Alloys with these compositions were melted in an arc furnace using a water-cooled container in a nitrogen atmosphere from a ligature of compositon Ti_2Ni, TiNi and $TiNi_3$ and graphite of high purity.

After annealing of the alloys at 1280°, metallographic analysis determined that all the alloys were

two-phase. One of the phases had a microhardness of about 3000 kg/cm^2.

During the metallographic analysis of the billets of melted titanium carbide obtained from titanium and carbon, there were clearly apparent graphite exclusions which were primarily located in the upper portion of the billet. Thus, during the process of melting the uncombined graphite is strongly liquated. Since the free energy of formation of titanium carbide is quite high -- at 2000° K it is 49 kcal/mol and continues to increase as the temperature is lowered, (Ref 11) -- while the free energy of formation of the solid solution of titanium carbide in nickel is much lower, the decomposition of titanium carbide by nickel would be accompanied by a large increase in the free energy of the system. Therefore such a process cannot occur spontaneously.

Table 1

The content of free and combined carbon in titanium carbide prepared by arc melting

Номер плавки (a)	$C_{общ}$, % (b)	$C_{своб}$, % (c)	Номер плавки (a)	$C_{общ}$, % (b)	$C_{своб}$, % (c)
1	20,2	0,8	5	20,3	1,4
2	19,8	0,6	6	20,1	0,5
3	20,1	0,6	7	19,9	0,6
4	19,9	0,7			

(a) melt number
(b) total carbon %
(c) free carbon, %

We also determined the solubility of nickel in titanium carbide. Alloys containing up to 30% by weight of Ni were prepared by hot pressing since it was not possible to obtain billets which were homogenous throughout the section by melting in the case of those alloys containing less than 10% Ni. The hot pressing was performed at temperatures of 2000-2200° for those samples which had a nickel content up to 5% while temperatures of 1900-1950° were used when the nickel content was 10-20%. The alloy containing 30% Ni was pressed at 1850°.

The solubility was determined by the quench method with metallographic analysis of the ground end after annealing under various conditions and with varied duration of annealing at 1700, 1650, 1280, 1200, and 1000°. It was found that the alloys containing up to 0.6-0.7% Ni are

single-phase at all temperatures, while with a higher nickel content a second phase appears which is a nickel-base solid solution.

The metallographic analysis data were confirmed by X-ray analyses using the method of negative photography of the test section. The X-ray pictures were taken using cobalt radiation with the 420 line focused. In order to determine precisely the position of the solidus line in the alloys rich in titanium carbide, differential thermal analysis was conducted on samples of the alloys containing 10-20% nickel after extended homogenizing annealing at 1250°. It was found that the initiation of melting in all of the samples occurred at 1280-1300°. The data obtained and the earlier published information (Refs 3, 7) permitted the construction of the phase diagram for the system TiC-Ni presented in Fig 3.

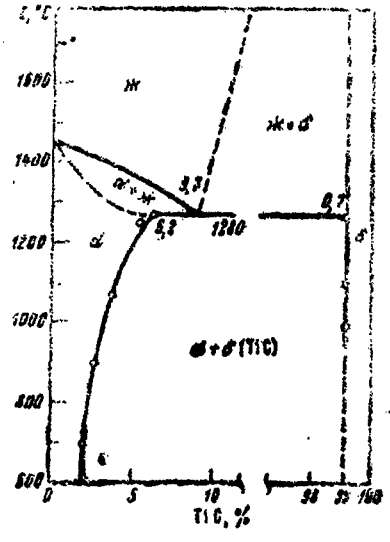

Fig 3. Phase diagram of the system TiC-Ni

THE TITANIUM-CARBON-CHROMIUM SYSTEM

A summary of data on the structure of the alloys of the system Ci-Cr is presented in Ref 4 and that for the system C-Cr in Ref 5.

There is very little data on the interaction of titanium carbide with chromium. Ref 1 indicates that in the alloys of titanium carbide with chromium there is a third phase which was identified by X-ray analysis as chromium carbide Cr_7C_3. Engel (Ref 15) also observed the interaction of chromium with titanium carbide during the melting of

chromium in containers made of sintered titanium carbide. The molten chromium scarcely penetrated between the grains of the titanium carbide and at the points of contact the formation of a new phase was observed.

During melting of chromium containing small (0.5% by weight) additions of technical carbide we also observed the formation of a new phase which was identified by X-ray analysis as the lowest cubic carbide of chromium, $Cr_{23}C_6$.

These observations are not in good agreement with the thermodynamic characteristics of the carbides. The free energy of formation of titanium carbide as noted previously is 49 kcal/mol at 2000° K. At this same temperature the free energy of formation of $Cr_{23}C_6$ per gram-atom of carbon is 16.2 kcal/mol (Ref 11). The corresponding magnitudes for TiC and Cr_3C_2 at 1500° K are 52.1 and 12.2 kcal/mol (Ref 16). To clarify how the system Ti-C-Cr is triangulated we prepared and studied the alloys whose composition is noted by the points 1,2 on Fig 4.

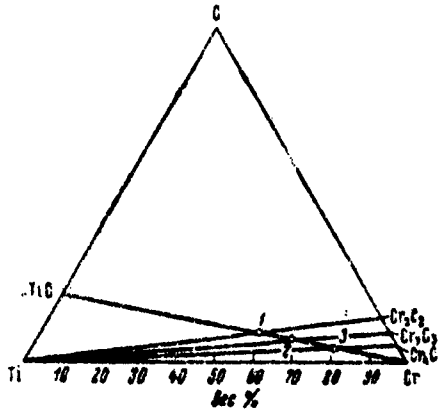

Fig 4. Composition of the alloys studied

These alloys were melted in an arc furnace from titanium and the chromium carbides Cr_3C_2 and Cr_7C_3, from titanium carbide and metallic chromium. In the preparation of the alloys we used Cr_7C_3 with 8.9% by weight of combined carbon (theoretical combined carbon being 9.06%) and Cr_3C_2 with 13.4% by weight total carbon and 0.16% by weight free carbon (theoretical combined carbon being 13.33%). The titanium carbinde contained 19.2% by weight of total carbon and 0.4% by weight of free carbon (theoretical combined carbon being 20.0%). The chromium contained 0.1 weight % of C. Samples were also prepared of alloys with 20 weight % of Cr from TiC and Cr of the noted composition as well as from titanium carbide with 19.7 weight % of

combined carbon and 0.05 weight % of free carbon.

Metallographic analysis of the samples of the alloys which had been annealed at 1200° indicated that the alloys prepared from chromium carbide and metallic titanium [See Note] and the alloys with 20 weight % of Cr which were melted from titanium carbide having 0.05 weight % of free carbon and 19.7 weight % of total carbon were two-phase. The microhardness of the phases (300 and 3000 kg/cm^2) corresponds to the hardness of the chromium base and titanium carbide base phases.

[Note. These alloys had the following compositions:
Alloy 1: 52.85% Cr; 36.9% Ti; 9.1% C (9.2% C theoret)
Alloy 2: 63.0% Cr; 20.5% Ti; 6.4% C (6.4% C theoret)
C theoret is the quantity of carbon which corresponds to the stoichiometric composition of titanium carbide based on the quantity of titanium found in the alloy by analysis.]

The alloys denoted by points 1 and 2 on Fig 4 and the alloys containing 20 weight % Cr prepared from titanium carbide having 0.4 weight % of free carbon and 19.2 weight % of total carbon were found to be three-phase. The microhardness of the phases in these alloys were 300, 1000, and 3000 kg/cm^2, which corresponds to the hardness of the chromium, chromium carbide, and titanium carbide bases. Such a difference in the structure of alloys prepared from titanium carbide with differing amounts of combined carbon is explained by the presence of admixtures of oxygen and nitrogen. We know (Refs 4, 17) that the presence of admixtures of oxygen and nitrogen make it impossible to obtain titanium carbide of stoichiometric composition. The formation of chromium carbides, as observed in Refs 1, 15 as well as in this present work, in the alloys prepared from titanium carbide of non-stoichiometric composition is caused by the presence of the impurities. For example, in the preparation of an alloy with 20% Cr from TiC having 19.2 weight % of total carbon and 0.4 weight % of free carbon 0.32 weight % of free carbon is introduced into the charge with the titanium carbide. This amount is sufficient to bind about 3 weight % of Cr in the carbide Cr_7C_3 and about 5 weight % of Cr in the carbide $Cr_{23}C_6$. The maximum energies of the reactions of the interaction of the titanium with the chromium carbides are characterized by the following magnitudes.

At 298° K:

$$Ti + \frac{1}{6}Cr_{23}C_6 + TiC \rightarrow \frac{23}{6}Cr \qquad A = -\Delta F = 40 \text{ kkal},$$

$$Ti + \frac{1}{2}Cr_7C_3 + TiC \rightarrow \frac{7}{2}Cr \qquad A = -\Delta F = 45.9 \text{ kkal},$$

$$Ti + \frac{1}{3}Cr_7C_3 + TiC \rightarrow \frac{7}{3}Cr \qquad A = -\Delta F = 41.9 \text{ kkal}.$$

At 2000° K:

$$Ti + \frac{1}{6}Cr_{23}C_6 \rightarrow TiC + \frac{23}{6}Cr \qquad \Delta F = -\Delta F = 32{,}7 \text{ kcal}$$

At 1500° K:

$$Ti + \frac{1}{2}Cr_3C_2 \rightarrow TiC + \frac{3}{2}Cr \qquad \Delta F = -\Delta F = 40{,}7 \text{ kcal}$$

These thermodynamic data indicate that the equilibrium of the reactions at temperatures from 298 to 2000° is shifted sharply towards the formation of titanium carbide, and consequently the system TiC-Cr is not reciprocal with the systems Ti-$Cr_{23}C_6$, Ti-Cr_7C_3, and Ti-Cr_3C_2. Thus, on the basis of this data we may conclude that the section TiC-Cr of the ternary system Ti-C-Cr is quasibinary.

THE TITANIUM-CARBON-MOLYBDENUM SYSTEM

A summary of the data on the system Ti-Mo is presented in Ref 4, and data for the system Mo-C in Ref 18. The latter also presents a little information on the ternary system Ti-C-Mo in the area of the triangle Mo_2C-TiC-MoC. Ref 2 has appeared recently giving the results of the investigation of the structure of the alloys of the ternary system Ti-C-Mo at 1710°. The authors did not set out to clarify the trend of the progress of the reactions in the system and the empirical data was not critically evaluated, so that the position of the phase fields in the isothermal section (Fig 5) presented in that work require revision.

Of the two compounds of the Mo-C system which are well known, Mo_2C and MoC, the monocarbide is stable only at high temperatures; at low temperatures it separates into Mo_2C and free carbon. Mo_2C is formed by a peritectic reaction. At a temperature of 298° K the energy of formation of Mo_2C is negative (Ref 11) with a magnitude of 2.8 kcal/mol. Fig 6 shows the variation with temperature of the logarithm of the activity of the carbon in titanium carbide and in molybdenum carbide, Mo_2C (Ref 11). The relative stability of these carbides is determined by the difference

$$\Delta F_{T(TiC)} - \Delta F_{T(Mo_2C)} = RT\left[\ln a_{C(TiC)} - \ln a_{C(Mo_2C)}\right]$$

As we see from Fig 6, this difference is essentially negative over the entire temperature range right up to the melting temperature of molybdenum carbide, i.e. TiC at all temperatures is far more stable than Mo_2C, although with a rise in temperature the values of ΔF_{TiC} and ΔF_{Mo_2C}

converge.

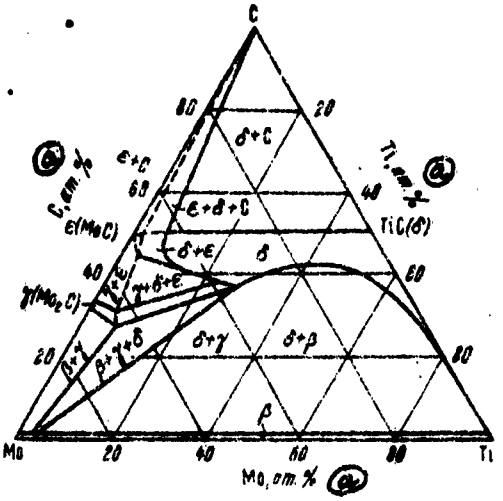

Fig 5. Isothermal section of ternary system Ti-C-Mo (Ref 2)
ⓐ atomic %

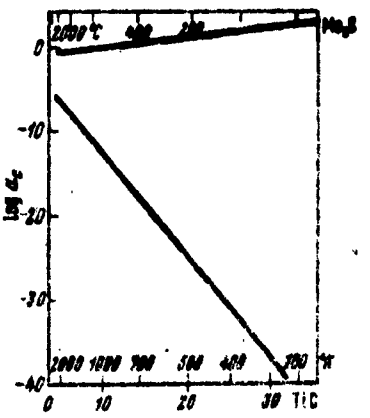

Fig 6. Carbon activity in TiC and Mo_2C vs temp.

This indicated that in the system Ti-C-Mo the equilibrium of the reaction

$$Mo_2C + Ti \rightarrow TiC + 2Mo,$$

and consequently also the reactions

$$MoC + Ti \rightarrow TiC + Mo,$$

$$2MoC + Ti \rightarrow TiC + Mo_2C$$

is sharply shifted toward the formation of TiC or solid solutions in a TiC base. From this we must conclude that the section Mo-TiC of the ternary system Ti-C-Mo must be quasibinary.

In order to experimentally prove the validity of this conclusion we prepared alloys lying on the intersection of the section Mo-TiC with the sections Mo_2Ti and MoC-Ti. In the preparation of the alloys, we used molybdenum, titanium, graphite, titanium carbide and Mo_2C (total carbon of 6% and free carbon of 0.15%). The charge for each alloy was formed by two means: from molybdenum and titanium carbide, and from titanium and molybdenum carbide. The alloys were made by sintering the samples in a vacuum of

10^{-4} mm Hg at a temperature of 1850° using high-frequency heating for 5 hours, followed by metallographic and X-ray analysis.

The metallographic analysis showed that all the alloys, regardless of which initial materials were used in the charge, consist of two phases with microhardness of about 300 and 2400 kg/mm^2. During X-ray analysis, in all of the samples only two phases were found: one a titanium carbide base and the other a molybdenum base, as illustrated in Fig 7. The alloys prepared by arc melting from titanium carbide of a stoichiometric composition and molybdenum of high purity were also two-phase for all ratios of the constituents and contained only TiC and molybdenum phases. Thus, the experimental data confirm that the section TiC-Mo is quasibinary.

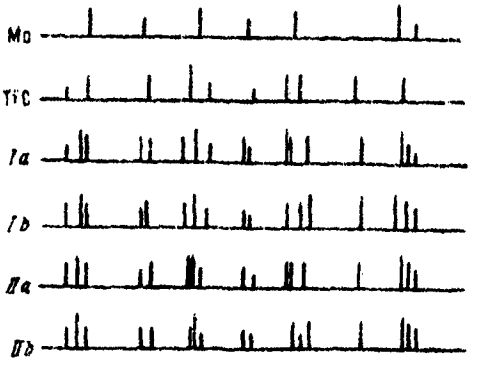

Fig 7. Line X-ray diagram of alloys of titanium carbide with molybdenum prepared by different methods

As a result of the proof that the section TiC-Mo is quasibinary, we must consider that the position of the phase fields in the isometric diagram (Ref 2), (Fig 5) is incorrect, since, in accordance with this diagram a considerable three-phase field appears in the section TiC-Mo with TiC, Mo_2C, and Mo-base phases. The existence of an extensive area of solid solutions of molybdenum in titanium carbide which was presented in Ref 2, and which has been confirmed by our investigations, does not contradict but rather confirms the quasibinary property of the section Mo-TiC, since

$$\Delta F_{(TiC,\ Mo)} < \Delta F_{(TiC)} + \Delta F_{(Mo)}.$$

but since

$$\Delta F_{(Mo)} = 0,$$

then

$$\Delta F_{(TiC,\ Mo)} < \Delta F_{(TiC)},$$

that is,

$$\Delta F_{TiC,\ Mo} - \Delta F_{(Mo_2C)} > \Delta F_{(TiC)} - \Delta F_{(Mo_2C)}.$$

CONCLUSIONS

1. The section TiC-Ni of the ternary system Ti-C-Ni is quasibinary.

2. The solubility of nickel in titanium carbide over the temperature range 1000-1220° is 0.7 weight % of Ni.

3. Points on the solidus in alloys of titanium with 10-20% Ni were determined, and a phase diagram of the quasibinary system TiC-Ni was drawn.

4. The sections TiC-Cr and TiC-Mo are quasibinary.

5. The phase fields in the system Ti-C-Mo as found in the work of Albert and Norton (Ref 2) are incorrect. More accurate experimental investigations are required in order to establish the boundaries of the phase fields of the system Ti-C-Mo.

REFERENCES

1. C.C. McBride, H.D. Grenhous, T.S. Shevlin. J. Amer. Ceram. Soc., 35, 28, 1952
2. H. Albert, J. Norton. Planseeberichte Für Pulvermetallurgie, 4, 2, 1956
3. E.R. Stover, J. Wulf. Trans. AIME, 215, 127, 1959
4. V.N. Yeremenko. Titan i yego Splavy (Titanium and its Alloys), USSR AS Press, 1960
5. M. Hansen, K. Anderko. Constitution of Binary Alloys, London, 1958
6. V.N. Yeremenko. Titan i yego Splavy (Titanium and its Alloys), USSR AS Press, 1955
7. V.N. Yeremenko. ZhNKh (Journal of Scientific Chemistry), 1, 2130, 1956
8. V.N. Yeremenko, T. Ya. Kosolapova. Voprosy Poroshkovoy Metallurgii i Prochnosti Materialov (Problems in Powder Metallurgy and Strength of Materials), 7, 3, 1959
9. R. Steinitz. J. Metals, 5, 891, 1953
10. V.N. Yeremenko, V.M. Polyakova, Z.P. Golubenko. Voprosy Poroshkovoy Metallurgii i Prochnosti Materialov (Problems in Powder Metallurgy and Strength of Materials), 3, 62, 1956
11. Physical Chemistry of Metals, London, 1953
12. V.N. Yeremenko, N.D. Lesnik. Voprosy Poroshkovoy Metallurgii i Prochnosti Materialov (Problems in Powder Metallurgy and Strength of Materials), 3, 73, 1956
13. A.N. Zelikman, D.S. Bernshteyn. Collection of Scientific Works, No 23, M.I. Kalinin Institute of Non-Ferrous Metals and Gold in Moscow and the All-Union Society of Metallurgists, State United Scientific and Technical Press, Moscow, 1952
14. V.N. Yeremenko, V.M. Bulanov, L.A. Gayevskaya. Chemical Review, Kiev State University Press, No 7, 1956
15. W.J. Engel. Metal Progress, 59, 664, 1951
16. O. Kubashevskiy, E. Evans. Termokhimiya v Metallurgii (Thermochemistry in Metallurgy), IL (Foreign Literature), 1954
17. G.A. Meyerson. Bulletins of Physical and Chemical Analysis, USSR AS, 16, 1, 1943
18. R. Kieffer, P. Schwarzkopf. Tverdye Splavy (Hard Alloys), State United Scientific and Technical Press, 1957

10,484
CSO: 1879-S

AN INVESTIGATION OF THE PRINCIPLES IN VIBRATION PRESSING OF POWDER METAL MATERIALS

[Following is the translation of an article by N. S. Gorbunov, I. G. Shatalova, V. I. Likhtman, and P. A. Rebinder in the Russian-language book Issledovaniya po Zharoprochnym Splavam (Research on Refractory Alloys), Vol 8, USSR Academy of Sciences Press, Moscow, 1962, pp 103-110.]

In the Soviet Union at the present time a new branch of industry -- powder metallurgy -- is growing at a rapid rate. The methods of powder metallurgy are used in the production of many machine parts, friction and anti-friction materials, copper-graphite compounds, magnetic materials, and products of the refractory and particularly of the hard materials. This method consists basically of the following technological steps: 1) preparation of the powders, 2) pressing of the briquettes, 3) sintering of the briquettes.

When it is necessary to produce compacted products from powders a high and uniform density of the briquettes throughout their volume is required. The existing methods of forming, such as static, hydrostatic, plasticized billets, jet extrusion, rolling, hot pressing, and others, cannot satisfy all the requirements imposed on the pressed billets or the final product. The fundamental task in the pressing of metallic powders is the attainment of a definite density and strength of the semi-processed material which will permit further technological operations and will ensure the required operational qualities of the product.

When using powders of the soft and plastic metals it is easy to control the porosity and strength during the pressing process by plastic deformation of the powder particles. In this case neither the granulometric composition of the powder nor the condition or relief of the surfaces of the particles will play a decisive role in establishing the mechanical properties of the semi-processed material. But the situation is quite different for the powders of the hard and brittle alloys. The particles of these powders do not have the capability of plastic deformation and consequently the density of the compact is determined only by the mould filling conditions and are only very slightly dependent on the pressing pressure, as long as it does not lead to fracture of the particles.

When the volume of the mould is uniformly filled the density of the compact is critically dependent on the granulometric state and reaches a maximum for semi-dispersed powders when the smaller particles are distributed in the spaces between the larger particles. However, the optimum distribution of the particles in the volume of the mould

cannot be obtained by simple static compression and the porosity of such compacts is always far from the optimum which corresponds to the correct (most dense) arrangement of the particles. The construction industry has long used modern methods for the compacting of materials with the aid of the low-frequency vibrating effect. This method is very effective and provides a maximum density of arrangement which is close to the theoretical value calculated from the granulometric composition of the powder. The mechanism of the favorable effect of low-frequency vibrations on the compacting process lies in the fact that the vibration destroys the initial point contacts which occur and thus leads to a more dense arrangement of the particles of the powder. These phenomena which accompany the process of vibration compacting must be present even at very low pressing pressures and consequently will not be accompanied with fracture of the particles. This is especially important for the powders of the hard and brittle materials.

As we mentioned, there are techniques for the compacting of materials by use of vibrating equipment (Refs 1, 4). Vibration is used for compact laying of concrete solutions with various fillers (Refs 2, 3) and for the compacting of subgrade and surfaces of highways, etc. Based on this experience we might expect that metallic and nonmetallic powders could also be successfully formed using vibration techniques (Ref 4).

This paper covers the investigation of the process of the vibration compaction of several materials in powder form. The vibration source used was a mechanical vibrator of the I-116 type having a frequency of 14,000 cycles/min and kinetic moment of 0.065 kg-cm. The vibrator was mounted on springs and developed amplitudes as high as 30 microns. The maximum amplitude developed by this type of vibrator when mounted on uncompressed springs is 10 microns. As the spring compression is increased the vibration amplitude increases to 30-40 microns and then drops sharply to 10-15 microns with a subsequent more gradual reduction. When pressing powders of various materials the magnitude of the change in the vibration amplitude as a function of the compression of the spring (and consequently of the pressure on the compact) is variable but the pattern of the change was the same for all of the materials studied.

In order to determine which materials are best suited to the vibration compaction method, 15 different powders were used; four metals, two carbides, six mixtures of a carbide with a metal, one nitride and two borides. A comparison was made of static and vibration methods of compac-

tion and the results are presented in Table 1.

A comparison of the magnitude of the relative density of the compacts produced using this method with the elastic modulus of the powder material indicated that the plastic materials with a low elastic modulus were compacted more poorly by the vibration method than by the usual static method. For materials having an elastic modulus from 25,000 to 50,000 kg/mm^2 the vibration method of compacting using a specific pressure of up to 20 kg/cm^2 produced the same density as did the static method using a specific pressure of 1200 kg/cm^2. Materials with elastic moduli above 50,000 kg/mm^2 were compacted better by the vibration method than by the static method. Thus, the application of vibration during compaction was most effective with the nonplastic materials.

Table 1

Материал порошка (a)	Модуль упругости, кг/мм^2·10^3 (b)	$\theta = \frac{\rho_к}{\rho_м}$		$\frac{\theta_{вб}}{\theta_{ст}}$
		$\theta_{вб}$ 0—30, кг/см^2	$\theta_{ст}$ 1200, кг/см^2	
Ti	11,7	38	51	0,74
Co	20,4	33	43	0,76
Cr	25,9	64	65,5	0,98
TiN	25,6	70	69	1,01
ZrB_2	35	54	53,5	1,01
Mo	33—37	65	63	1,03
TiB_2	37	52	50	1,04
TiC	46	84	75	1,12
WC	71	65	57	1,14
80% WC + 20% Co	50—53	53,5	55	1,01
94% WC + 6% Co	62—65	50	48	1,04
97% WC + 3% Co	68—70	60	57	1,05
96% [TiW]C + 4% Co (T30K4)	50	62	60	1,03
44% [TiW]C + 50% WC + 6% Co	53	65	61	1,07
15% [TiW]C + 75% WC + 10% Co	59	55	51	1,08

Note. $\theta_{вб}$ is the relative density of the vibrated sample, %; $\theta_{ст}$ is the relative density of statically compacted samples, %; $d_к$ is the density of the compact, g/cm^3; $d_м$ is the density of the compacted material, g/cm^3.

(a) powder material
(b) elastic modulus, kg/mm^2·10^3

Fig 1 presents the variation of the density of the compacts of cobalt and chromium powders as a function of the pressure on the powder during static and vibration compaction. The cobalt powder, which is capable of plastic deformation under pressure without fracture of the particles, produces better density when using the static method of compaction. For the less-plastic chromium powder the

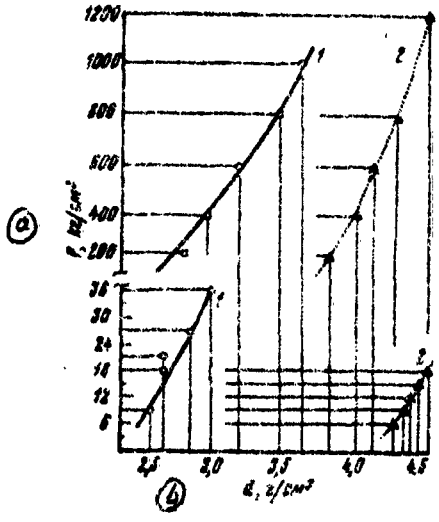

Fig 1. Density of compacts of cobalt (1) and chromium (2) powders as a function of pressure and method of pressing; upper curve, static lower curve, vibration (moistening agent is a 6% solution of glycerine in methanol, 10 cm^3 per 100 g)
ⓐ p, kg/cm^2
ⓑ d, g/cm^3

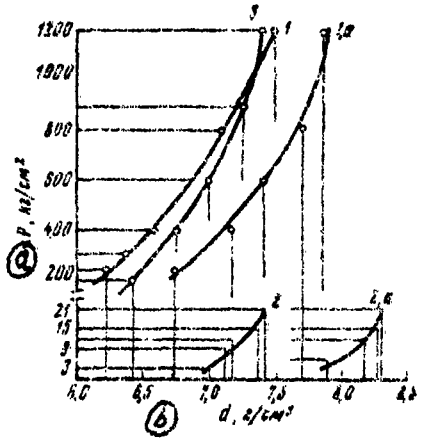

Fig 2. Density of compacts of a mixture of powders of tungsten carbide and 20% Co as a function of pressure and method of compaction; 1 - static, 2 - vibration, 3 - hydrostatic (moistening agent, water, 7 cm^3 per 100 g) 1a - static, 2a - vibration, 3a - hydrostatic (moistening agent is a 6% solution of glycerine in methanol, 10 cm^3 per 100g)
ⓐ p, kg/cm^2
ⓑ d, g/cm^3

vibration method provides a higher relative density than with the two other powders but it is still less effective than the static method, particularly if we consider that for pressures above 1200 kg/cm^2 the density of the chromium compacts is significantly increased without fracture of the briquette after removing it from the mould.

Curves 1-3 of Fig 2 present the variation of the density of the compacts prepared from a powder of a mixture of tunsten carbide and 20% by weight of Co as a function of the specific pressure during compaction by three methods: vibration, static, and hydrostatic. It was not possible to obtain compacts of tungsten carbide which were "transportable" without the use of a moistening agent so that there is no data on the variation of density as a function of pressure for that method. The most plastic material is a mixture of powders of tungsten carbide and 20% by weight of Co. It was less affected by the vibration method of compaction than the carbide but in order to obtain a mixture density of 7.3 g/cm^3 using the static method a pressure of 1200 kg/cm^2 was required while the vibration method required only about 15 kg/cm^2.

This difference becomes especially important when it is necessary to press products of complex shape from this mixture. The use of high pressures leads to cracking of the compacts in the areas of sharp changes in profile. The same is true of a mixture of tungsten carbide and 6% by weight of Co in powder form. For a mixture of tungsten carbide and 3% by weight of Co the vibration method permits the production of higher densities than with the static method since the application of specific pressures above 3000 kg/cm^2 in the static method leads to fracture of the compacts of any shape after removal from the matrix. It is not possible to obtain a density of 9 g/cm^2 using any lower pressures in the static method while this density may be achieved using the vibration method at specific pressure of 27 kg/cm^2. This effect is even more marked for the pure tungsten carbide powder (Fig 3, curves 1a, 2a). The density of 9.45 g/cm^3 obtained by the vibration method at a pressure of 5 kg/cm^3 cannot be obtained even at pressures above 1500 kg/cm^2 without vibration.

We investigated the variation of the density of compacts prepared from mixtures of the hard alloys of the types T30K4 (96%TiW + 4%Co), T15K6 (44%TiW + 50%WC + 6%Co), and T5K10 (15%TiW + 75%WC + 10%Co) as a function of the specific pressure during compaction by various methods.

Mixtures containing a high percentage of cobalt are less effectively compacted by the vibration method than mixtures with smaller cobalt content. The quantity of titanium carbide exerts the most influence on the modulus of elasticity in the listed mixtures but the capability to undergo vibration compaction is still determined by the quantity of the most plastic component -- namely cobalt. For all three mixtures the static and hydrostatic methods using specific pressures as high as 1200 kg/cm^2 was not

able to produce the density obtained by the vibration method at a pressure of 12 kg/cm^2, other conditions being equal.

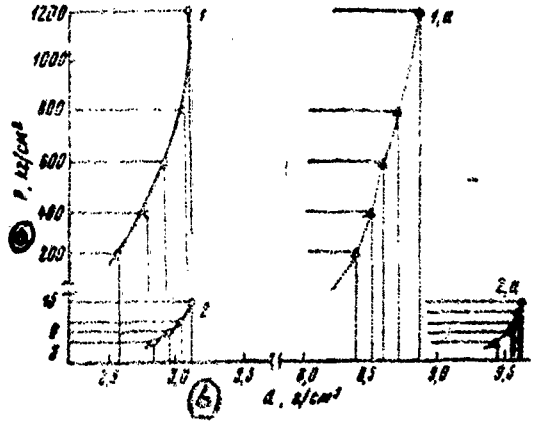

Fig 3. Density of compacts prepared from tungsten carbide and zirconium boride as a function of the pressure and method of pressing:
1a - static, 2a - vibration (moistening agent is water, 3 cm^3 per 100 g)
1 - static, 2 - vibration (moistening agent is water, 10 cm^3 per 100 g)
(a) p, kg/cm^2
(b) d, g/cm^3

In view of the poor pressing characteristics of the boride and nitride powders it was of interest to investigate their pressing using the vibration method. Curves 1 and 2 on Fig 3 present the variation of the density of compacts of zirconium carbide as a function of the specific pressure during static and vibration compaction and these curves are typical of those of the other materials of this group. The position of the curves indicate that the vibration method permitted the reduction of the pressure by a factor of 70 to 100 times. In addition, "transportable" compacts were obtained from all of the powders.

The powders which are well compacted by the vibration method do not require a long period of vibration to attain the maximum density. The variation of the density of the compacts as a function of time is presented on Fig 4. As can be seen, a rapid but not large increase in density during the first 3 seconds of vibration and a subsequent slow rise in density to the maximum value is characteristic

of the plastic powders. A sharp rise in density during the first 3-5 seconds (80-90% of the total rise) and a subsequent small rise to the maximum value during about 10 seconds is typical of the nonplastic powders. Further vibration will not lead to increase in the density. The shape of the density -- time curves as a function of the compacting pressure show that for all pressures in order to attain the maximum density of compacts of a mixture of 94% by weight of WC and 6% by weight of Co the same vibration time is necessary.

The density of the compacts obtained by vibration compaction are significantly dependent on the moistening agent and the quantity used. If we compare curves 1 and 1a, curves 2 and 2a in Fig 2 the following will be noted. In compaction of a mixture VK-20 (80%WC + 20%Co) by the vibration method, replacement of the water by a 6% solution of glycerine in methanol leads to an increase in density from 7.37 to 8.27 g/cm^3 at a pressure of 15.2 kg/cm^2 in comparison to a rise from 7.34 to 7.85 g/cm^3 at a pressure of 1200 kg/cm^2 using the static method. Thus, the lubricating action of the glycerine during the vibration method has much more effect than in the static method. By selection of the moistening agent it is possible to significantly improve the pressibility of the powders using the vibration method of compaction and as a result the vibration method becomes even more efficient (Ref 5).

For all of the powders studied an increase in the density of the compacts was noted for an increase in the quantity of the moistening liquid (Fig 5) up to a certain maximum which is well defined for each powder. With an increase in the compacting pressure this maximum shifts in the direction of a lower moisture content. If the density of the compact is less than 50% of the original powder the definite relationship of the density and moisture content is not observed.

The measurements made of the amplitude of vibration at varying specific pressure of compaction for the different powders led to the discovery of a relationship between the specific pressure on the powders, the amplitude of vibration, and the density of the compact. Assuming that the density varies in direct proportion to the frequency of vibration, the specific pressure, and the amplitude (within the limits of pressure and amplitude used in vibration compacting) we can find a compaction factor which to a certain degree characterizes the intensity of the effect of the vibrator on the powders. The results of such a mathematical analysis of the data for five different materials is presented in Table 2. The vibrocompaction

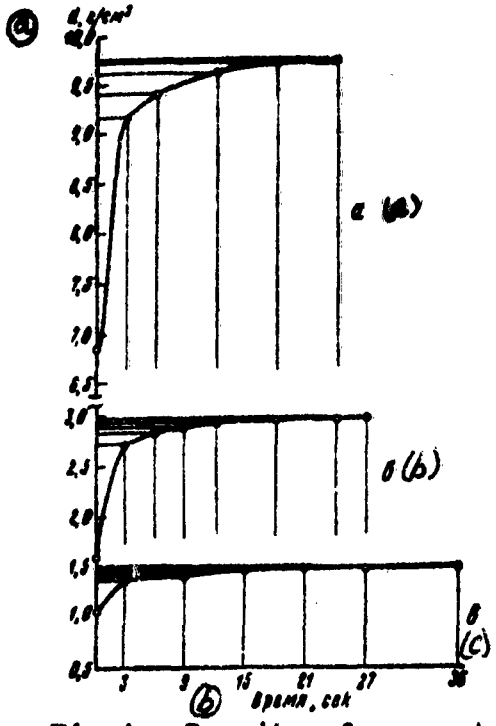

Fig 4. Density of compacts as a function of compacting time for powders of (a) tungsten carbide, (b) zirconium boride, (c) titanium
(a) d, g/cm^3
(b) time, sec

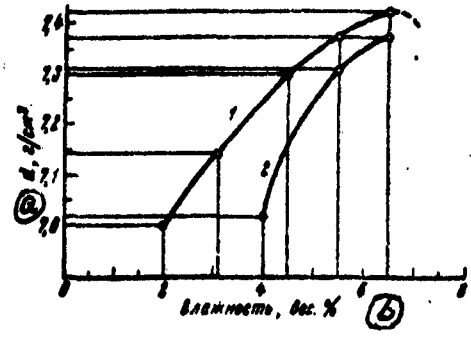

Fig 5. Density of compacts of a mixture of tungsten carbide and 20% Co powders as a function of the moisture content of the powders for vibration pressing:
1 - 6% solution of glycerine in methanol
2 - water
(a) d, g/cm^3
(b) moisture content, % by weight

factor ϕ is calculated as the product of the number of oscillations of the vibrator per minute, n, the specific pressure p_{sp} in kg/cm^2, and the amplitude of the oscillation of the lower end of the plunger, A, in cm, as found from the magnitude of the acceleration measured by an instrument of the PIU-1 type.

From the data of Table 2 it is clear that the variation of the magnitude of ϕ is in good agreement with the variation in density as a function of specific pressure in vibration compaction. For any one of the compacts we can read the indication of the accelerometer

Table 2

Cr, $d_к = 7{,}2$ г/см³						
(a) Давление, кг/см²	6,0	9,1	12,1	15,2	18,2	21,2
(b) Плотность, г/см³	4,33	4,40	4,45	4,54	4,56	4,30
Ф	110	130	276	396	437	374
Ti, $d_к = 4{,}5$ г/см³						
(a) Давление, кг/см²	8,0	15,8	20,0	26,3	31,6	40,0
(b) Плотность, г/см³	1,44	1,48	1,50	1,58	1,70	1,61
Ф	206	503	682	880	1030	595
Co, $d_к = 8{,}9$ г/см³						
(a) Давление, кг/см²	15,2	18,2	21,2	27,3	36,4	45,5
(b) Плотность, г/см³	2,50	2,58	2,60	2,80	2,95	2,89
Ф	328	415	482	750	948	535
80% WC + 20% Co, $d_к = 14{,}2$ г/см³						
(a) Давление, кг/см²	6,0	10,6	15,2	21,2	27,3	30,3
(b) Плотность, г/см³	7,9	8,17	8,27	8,29	—	—
Ф	113	241	340	417	543	415
WC, $d_к = 15{,}5$ г/см³						
(a) Давление, кг/см²	6,0	9,1	12,1	15,2	18,2	21,2
(b) Плотность, г/см³	9,45	9,56	9,58	9,61	9,62	9,56
Ф	110	177	283	361	361	332

(a) pressure, kg/cm^2 (b) density, g/cm^3

Table 3

(a) Тип вибратора	(b) Момент, кг·см	(c) Частота колебаний, колебаний/мин	(d) Плотность прессовки, г/см³
И-116, малая булава (e)	0,065	14000	7,15
С-623, малая булава (f)	0,10	14000	7,30
И-116, большая булава (g)	0,35	10000	7,85

(a) type of vibrator
(b) moment, kg-cm
(c) vibration frequency, cycles per min
(d) density of compact, g/cm^3
(e) I-116, small rod
(f) S-623, small rod
(g) I-116, large rod

as a function of the specific pressure on the powder and we can find the optimum pressure for vibration compaction of the given powder.

The possibilities of the use of the vibration technique in the preparation of parts from the metallocermic materials and refractory metals are of great interest. Table 3 present the variation in density of compacts made from a powder of the mixture VK-20 (80%WC + 20%Co) as a function of the mechanical properties of the vibrator.

The data of Table 3 show that as the kinetic moment increases from 0.065 to 0.35 kg-cm the density of the compact increases. However, the most powerful of the available vibrators is inadequate to compact as much as 60-70% of a part which is 50-100 mm tall and has a cross-sectional area of 5-10 cm^2. This means that at the present time and using available equipment for vibration compacting we have the capability of pressing by this new method parts with heights to 20 mm and areas up to 10 cm^2. Existing vibrators for the compaction of concrete aggregates have a kinetic moment of 20-30 kg-cm but their frequency is less than 6000 cycles per min and the amplitude is too great for powders with particles of 10 microns and smaller. Experience in the compaction of concrete aggregates has also shown that for aggregates with small particles the optimal frequency is 6,000 to 30,000 cycles per min and has indicated the harmful effects of large amplitudes.

Our investigations have shown that more powerful vibrators having higher frequencies (10,000 to 20,000 cycles per min) and specially designed vibration presses are required for the wide application of vibration compaction to the metallocermic and refractory powders.

REFERENCES

1. V.I. Likhtman, N.S. Gorbunov, I.G. Shatalova, P.A. Rebinder Doklady ANSSSR (Reports of the USSR AS), 135, 5, 1960
2. N.V. Mikhaylov, P.A. Rebinder. Arkitektura (Architecture), 9, 1960
3. A.E. Desov. Vibrirovannyy Beton (Vibrated Concrete), Glavstroyizdat, 1956
4. W.C. Bell, R.D. Dellender. J. of the Am. Cer. Soc., No 11, 1955
5. V.I. Likhtman, P.A. Rebinder. Doklady ANSSSR (Reports of the USSR AS) 70, 3, 1950

16,484
CSO: 1879-S

CERTAIN PROBLEMS IN THE THEORY OF THE THERMAL SHOCK RESISTANCE OF POWDER METAL MATERIALS

[Following is the translation of an article by M. Yu., Bal'shin, and V. I. Likhtman in the Russian-language book Issledovaniya po Zharoprochnym Splavam (Research on Refractory Alloys), Vol 8, USSR Academy of Sciences Press, Moscow, 1962, pp 110-116.]

The improved thermal shock resistance of powder metal materials in comparison with cast materials of the same composition has been noted in numerous works (Refs 1, 2, 3). This paper is devoted to a more detailed investigation of the nature of the thermal shock resistance of the powder metal materials and the factors bearing on the magnitude of this quantity.

First, it should be noted that the thermal shock resistance is a property of the end products and not of the materials themselves. It is difficult to find any other property as critical in structural design as thermal shock resistance. Thermal shock resistance is defined as the ability of a material (more precisely the products made from this material) to withstand cracking during several cycles of temperature change. Under identical conditions of thermal cycling, a large part will be subjected to more significant temperature differences in various sections than will a small part. For this reason the tensions caused by the temperature differences will also be greater in a large part so that under identical thermal cycling the large part will inevitably have more tendency to cracking than a small part. For example, in one of our series of experiments the increase in the diameter of a cylindrical sample by 25% (from 12 to 15 mm) led to a considerable decrease in the thermal shock resistance of the material which contained Cr_3C_2, TiC, and graphite.

During the temperature cycles which involved rapid heating to 1200° and quenching in water, the smaller samples withstood 17 cycles before developing cracks while the large samples withstood 40% fewer cycles. The initial electrical resistance of cylinders made from TiC-Cr_3C_2 having a diameter of 12 mm and a height of 18 mm after 4 cycles (rapid heating to 1000°, quench in water) had increased by 7.3 times while cylinders of the same material having a diameter of 15 mm and a height of 22 mm had experienced an increase of 10.5 fold. In this case an increase in the dimensions led to a decrease in the thermal shock resistance. It should be noted that in all the experiments the larger parts invariably had lower thermal shock resistance as shown by cracking and failing after fewer cycles and by a greater increase in the initial

electrical resistance per cycle (a reduction of the initial contact surface between the structural elements).

The shape factor which influences the concentration of stresses and therefore the thermal resistance was found to be quite significant. For example, the rounding of sharp edges of the cylinders always led to an increase in the thermal shock resistance of the samples. Even in the case of identical stresses caused by the cyclic variations of temperature, the larger parts should be less resistant to thermal shock.

Let us consider the case where the part undergoes a reversible deformation in some direction of ± 0.1% under sharp cyclic temperature changes. If the dimension of the body in this direction is 10 mm, then the total deformation in this direction will be ± 10 microns. Thus, the reversible deformation in the body may become irreversible if a crack with a lateral dimension of 10 microns is formed. As a rule the cracks due to cyclic temperature changes are formed between the structural elements of the material and not within them. This is particularly true of powder materials having incomplete mutual contact between the structural elements. If the dimension of the structural elements in the body under consideration is 1 micron, then the conditions favor the formation of inter-particle cracks (the total deformation is 10 microns and the thermal shock resistance of the body will be negligible). However, if the dimension of the structural elements were 100 microns then the formation of inter-particle cracks would be more difficult and the thermal shock resistance of the body would be considerably greater. If the body dimension is 1000 mm, the deformation per cycle would be ± 1000 microns. In this case even if the dimension of the structural elements is 100 microns inter-particle cracks may easily be formed and the thermal shock resistance of the body will be very low.

Thus, the thermal shock resistance of a body will increase to a certain degree with a decrease in the body dimensions and will increase with an increase in the dimensions of the structural elements of the body. This body dimension relationship always hold true regardless of the absolute dimensions of the body. In regard to the structural elements of the body, the increase in thermal shock resistance with increasing dimensions of the structural elements is valid only up to certain limits. In the case of very large structural elements failure under thermal cycling may occur within these elements which leads to their division into smaller structural elements. Thus, beginning with some limiting size at which the thermal

cycling causes failure within the structural elements rather than between them, further increase in the dimensions of the structural units is not helpful. Moreover, it may be harmful for the following reasons:

1) fracture of the structural elements may be accompanied by a definite orientation of the newly formed smaller elements in accordance with the temperature gradient which may seriously reduce the thermal shock resistance;

2) the bond between the large structural particles in many cases is weaker than that between the smaller particles and increases the tendency to cracking;

3) the thermal shock resistance is further reduced because of the coarsening of the pores during the increase in the dimensions of the structural elements.

Thus, there is a definite size of the structural elements below which an increase in dimensions (either simple or complex) leads to an increase in the thermal shock resistance of the material and above which an increase in dimensions causes degradation.

The following basic factors leading to significant improvement in the thermal shock resistance of the powder metals in comparison with the case metals should be noted.

1) the structural elements of the powder metals possess "individual" characteristics to a significantly higher degree than the grains of cast metals. This improves the resistance of the material to cracking under deformation and consequently improves the thermal shock resistance. For example, a stack of unglued paper sheets may be easily bent without any failure while the same stack of well-bonded sheets will fail when bent.

2) in Ref 1 it was shown that finely-dispersed pores can increase the thermal shock resistance and that fine spherical pores are particularly favorable.

3) the possibilities of regulating the structure in cast metals is much more limited than in the powder metals. For example, the structural elements in the powder metal materials can be either simple, as the grains of the cast metal, or complex.

These complex structural elements are aggregates of particles which may in turn be subdivided into grains. There are definite advantages to the production of powder products from these complex structural aggregates rather than from particles. The pores between these coarse structural aggregates are smaller than those between simple particles of the same dimensions and the strength of the bonds between these aggregates is greater than between particles of the same size. The strength of the bond between the particles within the aggregate are as a rule greater

Fig 1. A sample of aggregated sheet (parallel to the axis of forming) (x10)

than between simple particles of the same size (for identical conditions of preparation of the part).

There are several types of such aggregates. Equiaxed aggregates of particles (granules) were first described by one of the authors in 1938 in Ref 4. Another type is that of the fibrous aggregates which can be obtained by the processing of plasticized mixtures of powders in special centrifuges (Ref 5) or by extruding the plasticized mixture through a filter, a meat grinder sort of device, etc. The third type is sheet rolled from plasticized powder (Fig 1). From such sheet it is possible to form products by simple winding of the sheet with subsequent sintering, by cold pressing after winding and later sintering, or by hot pressing.

It is known that a thin-walled shell is much more resistant to thermal shock than a thick-walled cylinder. The structure of the sheet shown in Fig 1 is a sort of a thick-walled cylinder consisting of more or less individually separated thin-walled shells. Material with such a structure, as might be expected from theoretical considerations and as has been demonstrated by our experiments, is much more resistant to thermal shock than the usual powder or cast materials.

Thus the methods of powder metallurgy present great possiblities for the control of the structure which may be looked upon as a sort of "internal framework" of the product.

In our work we did not attempt to investigate the influence of the composition on the thermal shock resistance. However, the experiments were conducted with materials having different compositions in order to confirm the generality of the relationships derived. In order to reduce the time required for the experiments the com-

positions included some having low thermal shock resistance.

Table 1 presents the mean results of the experiments on the effect of the degree of aggregation of material in equiaxed granules. The initial particle dimensions were of the order of a few microns. The material was mixed in methanol in a ball mill for a period of 36 hours. After drying, part of the material was subjected to direct hot pressing in cylinders of 15 mm diameter and 12 mm height. Another part was mixed with a solution of rubber in benzene in order to obtain granules of the necessary dimensions. Part of the granules were subjected to a preliminary annealing at 1600° for 3 hours. All the materials were subjected to hot pressing at 2200° under a pressure of 50 kg/cm^2.

Table 1

TiC-Cr_3C_2-Graphite, mixed for 36 hours

Размер гранул, мк (a)	Назначенные гранулы (b)		Спеченные гранулы (c)	
	удельный вес (d)	число теплосмен * (e)	удельный вес (d)	число теплосмен (e)
Не гранулированные частицы до 10 (f)	3,98	0,5 (неполный цикл) (g)	—	0,5
125	3,68	9,7	3,81	13,5
160	3,82	10,3	4,03	17,7
200	3,77	5,3	3,76	14,0
250	3,80	8,4	4,12	9,3
315	3,68	7,9	3,78	11,0
350	4,01	10,3	3,92	11,3

(a) granule dimension in microns
(b) unsintered granules
(c) sintered granules
(d) specific weight
(e) number of temperature cycles
(f) non-granulated particles up to
(g) incomplete cycle
(h) from 1200° into water

Table 1 shows that the non-granulated form of the material had no thermal shock resistance. Granulation of the material increased the thermal shock resistance by 10-35 times, or more than an order of magnitude. There is an unclearly defined optimum granule size at about 160 microns. The better sintered granules had a thermal shock resistance from 1.1 to 2.6 times higher than the material formed from the unsintered granules.

Table 2

TiC-Cr_3C_2-Graphite, sintered granules, mixed for 18 hours

Размер гранул, мк (a)	Гранулы из карбидов, не подвергнутых вибропомолу (b)		Гранулы из карбидов, подвергнутых вибропомолу (c)	
	удельный вес (d)	число теплосмен (e)	удельный вес (d)	число теплосмен (e)
Не гранулированы	3,0	0,5	3,85	0,5
125	4.13	8,5	4,14	10,5
160	4,07	12	3,85	14
200	3,82	10	3,85	13,5
315	3,91	10,5	3,85	11,5
350	3,79	7	3.80	11
350	3,80	7	3,85	10

(a) granule dimension in microns
(b) carbide granules not subjected to vibromilling
(c) carbide granules subjected to vibromilling
(d) specific weight
(e) number of temperature cycles

Table 2 presents the mean results of the effect of vibromilling on the thermal shock resistance. It is clear that the preliminary vibromilling raised the thermal shock resistance of the granulated material by 20-50%. In addition, this series of experiments confirmed the data of Table 1 on the favorable influence of granulation on the thermal shock resistance.

Table 3 presents the results of the experiments on the effect of the homogeneity of the composition of the granules. In this series of experiments two types of granule were compared: 1) a homogenous composition, 2) a mixture of TiC + Cr_3C_2 with granules containing graphite. The data of Table 3 show that the composition of granules of the first type were 30-40% more resistant to thermal shock.

Table 4 shows the favorable effect on thermal shock resistance of extended milling of the initial mixture and Table 5 shows the effect of granulation and of strength of the granules for a composition having a higher resistance to thermal shock, SiC-B_4C-Grephite. The strength of the granules increasee progressively with increased moistening of the charge with benzine, bonding with rubber, bonding with bakelite, and sintering of the granules. It is clear from Table 5 that as the strength of the granules is raised the resistance to thermal shock of the composition is improved. As the strength of the granules is raised their optimum size is raised. For example, for the weakest

granules obtained by moistening with benzine the optimum thermal shock resistance is found for granules of 160 microns while for the stronger (bonded) granules the optimum is at 315 microns, and for the strongest (sintered) granules the optimum is at 350 microns.

Table 3

TiC-Cr_3C_2-Graphite

(a) Размер гранул, мк	(b) Гранулы TiC + Cr_3C_2 + C		(c) Гранулы отдельно TiC + Cr_3C_2 отдельно C	
	(d) удельный вес	(e) число теплосмен	(d) удельный вес	(e) число теплосмен
160	3,97	10,0	3,74	7,0
350	3,86	8,2	3,89	6,2
(f) 75% по весу 350 и 25% по весу 160	4,20	11,3	4,12	7,8

(a) granule dimension in microns
(b) granules
(c) granules of TiC + Cr_3C_2 and separate granules of C
(d) specific weight
(e) temperature cycles
(f) 75% by weight of 350 and 25% by weight of 160

Table 4

TiC-Cr_3C_2-Graphite

(a) Размер гранул, мк	(b) Размол 18 час.		(c) Размол 3 час.		Примечания (f)
	(d) удельный вес	(e) число теплосмен	(d) удельный вес	(e) число теплосмен	
Не гранулировано (g)	3,90	0,5	4,82	0,5	
125	3,81	7,3	3,88	8,0	(h) Неспеченные гранулы
160	3,90	9,0	4,66	12,0	
800	3,8	8,5	3,64	0	
315	3,6	6,5	3,64	10,3	
350	3,76	6,0	3,73	9,0	
350	3,70	5,0	3,74	[illegible]	
125	3,63	9,0	3,91	12,0	
160	3,65	9,5	4,0	12,5	Спеченные гранулы (i)
200	4,0	9,5	3,8[illegible]	10,5	
315	3,85	11,0	3,72	11,5	
350	3,81	10,5	3,73	11,5	
350	3,81	8,0	3,83	10,5	

(a) granule dimension in microns
(b) milled for 18 hours
(c) milled for 3 hours
(d) specific weight
(e) number of temperature cycles
(f) remarks
(g) not granulated
(h) unsintered granules
(i) sintered granules

Table 6

SiC-B_4C-Graphite

Размер гранул в микронах (a)	Смачивание бензином (b)		Склеивание каучуком (c)		Склеивание бакелитовым лаком (d)		Спеченные гранулы (e)	
	удельный вес (f)	число температур (g)	удельный вес (f)	число температур (g)	удельный вес (f)	число температур (g)	удельный вес (f)	число температур (g)
125	1,90	3	2,06	3,3	1,97	3,5	2,12	5,2
160	2,02	6,2	1,95	8	1,92	8,5	2,06	8,9
200	1,99	4	2,04	9,4	2,15	12,8	2,05	13,1
315	1,92	3,5	1,97	10,2	1,98	13,2	1,95	14,8
350	2,02	2,5	2,10	7	2,06	11,3	1,94	15,2

(a) granule dimension in microns
(b) moistened with benzine
(c) bonded with rubber
(d) bonded with bakelite varnish
(e) sintered granules
(f) specific weight
(g) number of temperature cycles

Table 6 presents the data from the testing of samples of unsintered sheet oriented parallel to the axis of forming of the sample (Fig 1), of unsintered foils oriented perpendicular to the axis (Fig 2), and of unsintered granules. The resistance to thermal shock of the samples formed from foils having an open surface and oriented perpendicular to the axis of forming was low. The samples of sheet having a closed surface and oriented parallel to the axis of forming had the highest reistance to thermal shock.

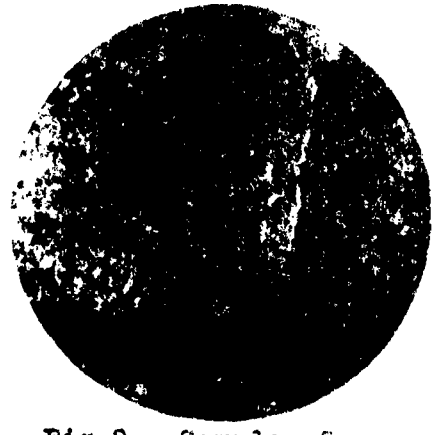

Fig 2. Sample of aggregated foils (perpendicular to the axis of forming) (x4)

We also compared samples prepared from fibrous granules with samples from equiaxed granules. The samples from aggregated fibre containing TiC, Cr_3C_2 and graphite withstood 15 temperature cycles while samples of the same composition with equiaxed granules withstood only 11 cycles. The electrical resistance of samples prepared from aggregated fibre increased only about 2/3 as much per temperature cycle as did the resistance of the samples prepared from equiaxed

granules.

The observed data are in agreement with the general principles of physical and chemical mechanics developed by P.A. Rebinder in Ref 6.

Table 6

TiC, Cr_3C_2, Graphite in unsintered granules

Original material	Sp Wt	No of temp cycles
Foils, oriented perpendicular to the forming axis (Fig 2)	3.76	1.3
Sheets, oriented parallel to the axis of forming (Fig 1)	3.91	12.5
Uniform granules-250 microns	3.82	8.7

CONCLUSIONS

1. The mechanism of the thermal shock resistance of the powder metal was investigated.

2. Preliminary granulation (aggregation) of the powders significantly increases the resistance to thermal shock.

REFERENCES

1. M.Yu. Bal'shin. Issledovaniya po zharoprochnym splavam (Research on Refractory Alloys), Vol 3, Izd. AN SSSR (USSR AS Press), 1958
2. Spravochnik po mashinostroitel'nym materialam (Handbook on Machine Construction Materials), Vol 2, 1959
3. M.Yu. Bal'shin. Osnovy tsvetnoy metallurgii (Principles of Non-Ferrous Metallurgy), Metallurgizdat (Metallurgy Press), 1960
4. M.Yu. Bal'shin. Patent No 76264, 1952
5. I.S. Brokhin, D.L. Federmeyer. Compendium, Tverdye splavy (Hard Alloys), Moscow, 1959
6. P.A. Rebinder. Fisiko-khimicheskaya mekhanika (Physical and Chemical Mechanics), Izd. AN SSSR (USSR AS Press), 1957

10,484
CSO: 1879-S

VISCOUS FLOW IN THE SINTERING OF POWDERS BY HOT PRESSING

[Following is the translation of an article by M. S. Keval'chenko, and G. V. Samsonov in the Russian-language book Issledovaniya po Zharoprochnym Splavam (Research on Refractory Alloys), Vol 8, USSR Academy of Sciences Press, Moscow, 1962, pp 116-126.]

The growing application of materials of high melting point, extreme hardness, high temperature resistance, and resistant to the action of various corrosive media in numerous areas of modern technology is related to the use of the refractory metals and combinations of these metals with nonmetals such as carbon, boron, nitrogen, and silicon (carbides, borides, nitrides, and silicides).

The high melting points of the refractory metals and compounds as well as the tendency of some of them to dissociate upon melting leads to the requirement for production in the form of powders with the subsequent transformation into compacted products by means of the powder metallurgy techniques. There are two basic methods used in this process: cold pressing of billets with subsequent sintering, and simultaneous pressing and sintering of the powders (hot pressing).

The latter technique produces a fine-pore product from the high-melting point, hard, and brittle metals and compounds with a minimum expenditure of time (Refs 1,2).

As shown in Refs 3-6, during sintering of the powders in the solid phase there is viscous or plastic flow of the material under the action of capillary pressure acting within the pores equal to $2\sigma/r$, where σ is the surface tension and r is the radius of the pore. A higher rate of compaction during the sintering of the powders by hot pressing in comparison with conventional sintering (without external pressure) is due to the capillary pressure being supplemented by the external pressure (Refs 7,8).

Based on models of closed spherical separated pores and on the conclusions of the phenomenological theory of sintering of MacKenzie and Shuttleworth (Ref 6), the authors of Ref 8 proposed the following equation for the rate of compaction of the material during hot pressing:

$$\left(\frac{d\rho}{dt}\right)_p = \left(\frac{d\rho}{dt}\right)_c + \frac{3}{4}\frac{P}{\eta}(1-\rho), \qquad (1)$$

where ρ is the relative density of the sintered body, that is the ratio of the density of the porous material to the

density of the particles forming it; t is time; P is the external pressure; η is the coefficient of shear (laminar) viscosity of the compacted material.

The subscripts $г$ and c correspond to the rate of compaction during hot pressing and during conventional sintering.

This equation, ignoring the first term on the right, i.e. on the assumption that $P \gg \frac{2\sigma}{r}$, was used in Ref 9 to determine the coefficient of viscosity of aluminum oxide at sintering temperatures. However, as we shall show later, this determination is invalid since equation (1) does not give satisfactory agreement with the experimental data (Refs 10,11).

This paper presents the phenomenological view of the process of compaction of the material during the sintering of powders by hot pressing in light of the mechanism of the viscous flow of crystalline bodies.

A porous body during the sintering in the solid phase is a mixture of practically incompressible solid particles and absolutely compressible voids which results in a marked compressibility (Ref 12). As a result of the chaotic distribution of the solid particles and the pores through the volume of the porous body, the latter may be considered isotropic, taking into account the degree of porosity by the coefficient f which is equal to the ratio of the volume of the pores V_2 to the total volume of the material $V = V_1 + V_2$, where V_1 is the volume actually occupied by the solid particles.

The overall specific volume of the body V and the volume of the pores V_2 may be expressed in terms of the specific volume of the solid particles V_1 forming the body since:

$$\frac{1}{f} = \frac{V_1 + V_2}{V_2} = \frac{V_1}{V_2} + 1. \qquad (2)$$

Whence

$$V = \frac{V_1}{1-f}; \quad V_2 = \frac{V_1 f}{1-f}. \qquad (3)$$

From the macroscopic point of view the process of the sintering of powders by hot pressing may be described as the process of the three-dimensional viscous flow of a porous body under the action of the forces of surface tension and the applied external pressure. Since this process is accompanied by a reduction of the volume (shrinkage), we may assume that the deformation of pore

shear is equal to zero.

During the compaction process as the porosity is reduced the sintered body will "thicken". This gradual thickening is described by the variation as a function of porosity of the second coefficient of viscosity ζ which enters into the equation of the hydrodynamics of viscous fluids (Ref 15). This coefficient, suggested in Ref 14, is given by the expression

$$\zeta = \eta_0 \frac{(1-f)(1-2f)}{f(1-f)}, \qquad (4)$$

where η_0 is the first coefficient of viscosity or the shear viscosity of the compacted material.

The relation between the rate of compaction and the applied forces may be found by equating the work of the external forces to the work of the internal friction forces as suggested by Ya.I. Frenkel' (Ref 3).

The work done by the external forces, referred to unit volume and unit time, is equal to the sum of the work performed by surface tension, $\frac{\sigma}{V}\frac{dS}{dt}$ (where S is the total surface of the pores) and by the applied pressure, $\frac{P}{V}\frac{dV}{dt}$.

The work performed by the dissipative forces of internal friction, referred to unit volume and unit time, may be expressed by the square of the dissipative function (Ref 13), which for the case of large volumetric deformations (Ref 15) takes the form

$$2\Psi = \zeta\left(\frac{dV}{V\,dt}\right)^2, \qquad (5)$$

where Ψ is the dissipative function and V is the instantaneous volume of the body.

Equating of the work of the external and dissipative forces leads to the equation

$$\zeta\left(\frac{1}{V}\frac{dV}{dt}\right)^2 = -\frac{\sigma}{V}\frac{dS}{dt} - \frac{P}{V}\frac{dV}{dt}. \qquad (6)$$

In order to reduce the number of variables in this equation we will express the surface area of the pores in terms of their volume. The surface area s_2 of a single pore having, for example, a spherical shape may be expressed in terms of its volume as follows:

$$s = 4\pi r^2,$$

It is clear that an analogous relation with a coefficient differing from 6 will hold for a pore of any shape.

Then the rate of contraction of the surface of the pore may be expressed by the equation:

$$\frac{dv_1}{dt} = \frac{dv_2}{dv_2}\frac{dv_2}{dt} = 4v_2^{-1/3}\frac{dv_2}{dt}.$$

Considering that the total surface of the pores is equal to the sum of the surface areas of the individual pores, the rate of contraction of the total surface of the pores of the sintered body may be written in the form:

$$\frac{dS}{dt} = \frac{d(nv_1)}{dt} = \frac{4}{v_2^{1/3}}\frac{d(nv_2)}{dt} = \frac{4}{v_2^{1/3}}\frac{dV_2}{dt},$$

where V_2 is the total volume of the pores and n is the number of pores in the volume V.

Since v_2 is equal to the linear dimension of the pore d_2, and in light of equation (3)

$$nd_1^3 = \frac{nd_2^3 f}{1-f} \text{ и } d_2 = d_1\sqrt[3]{\frac{1}{1-f}},$$

where d_1 is the linear dimension of the particles, then

$$\frac{dS}{dt} = \frac{4}{d_1}\frac{(1-f)^{1/3}}{f^{1/3}}\frac{dV_2}{dt}. \qquad (7)$$

Substituting into equation (6) the value of ζ from expression (4) and dS/dt from formula (7), expressing the total volume V and the volume of the pores V_2 in terms of the volume V_1 from formulae (3), we obtain the desired relation for the rate of change of porosity as a function of the external force acting on a porous body:

$$4\eta\frac{1-f}{f(3-f)}\frac{df}{dt} = -P - \frac{4\sigma(1-f)^{1/3}}{d_1 f^{1/3}}. \qquad (8)$$

For the case of the sintering of powders by hot pressing, the second term on the right in equation (8) may be neglected for the sake of simplification. The basis for this is that, for P of 100 kg/cm^2 or 10^8 dynes/cm^2, d_1 of 10 microns and the maximum possible value of σ of 2000 dynes/cm, the quantity

$$\frac{4\sigma}{d_1} \approx \frac{4\cdot 2000}{10^{-3}} \approx 8\cdot 10^6 \frac{\text{дин}}{\text{см}^2} = 8\ \frac{\text{кг}}{\text{см}^2}$$

constitutes only 10% of P. With an increase in the external pressure the contribution of the surface tension to the rate of compaction will decrease. Therefore, integrating equation (8) without the second term on the right and

determining the constant of integration from the condition $f = f_0$ for $t = 0$, we obtain:

$$\frac{1}{3}\ln f - \frac{5}{3}\ln(3-f) - \frac{1}{3}\ln f_0 + \frac{5}{3}\ln(3-f_0) = -\frac{P}{4}\int_0^t \frac{dt}{\eta}. \qquad (9)$$

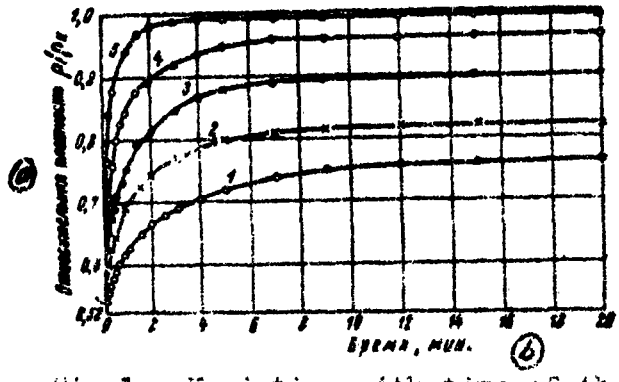

Fig 1. Variation with time of the relative density of samples of tungsten carbide under a pressure of 165 kg/cm^2 for temperatures of: 1 - 2100, 2 - 2200, 3 - 2300, 4 - 2400, 5 - 2500° (a) relative density (b) time, min.

Multiplying both sides by -1 and introducing the notation

$$F(f) = -\frac{5}{3}\ln(3-f) - \frac{1}{3}\ln f_0 + \frac{5}{3}\ln(3-f_0) + \frac{1}{3}\ln f_0, \qquad (10)$$

we write equation (9) in the more compact form:

$$F(f) = \frac{P}{4}\int_0^t \frac{dt}{\eta}. \qquad (11)$$

The quantity F(f) is the measure of the increase in density of powders during sintering by hot pressing. For η = constant, which is valid for Newtonian bodies, for example glass or resin, equation (11) takes the form

$$F(f) = \frac{Pt}{4\eta}. \qquad (12)$$

In order to compare equation (12) with experimental values, we analyzed the data of Williams (Ref 10) obtained during the sintering of glass powder under pressures of 40 and 80 kg/cm^2. The values of the reduced change in porosity F(f) calculated by formula (10) varied linearly with the time of sintering (Fig 1), which confirms the qualitative agreement of equation (12) with the experimental data.

The slope of the lines was used to calculate the value of the viscosity of the glass (the glass composition was not indicated in Ref 16) at a temperature of 600°. The value was found to be 7.86×10^{10}, which is of the order of magnitude of the handbook values. However, with the assumption that η is constant, equation (12) is not applicable to the described process of the sintering of powders of crystalline materials since in this case there is considerable deviation of the experimental values of F(f) from the linear relation given by equation (12). For this reason we must presume that the sintering of crystalline powders takes place in conditions of unsteady flow wherein the coefficient of shearing viscosity of the crystalline bodies depends on the duration of sintering.

As shown in Refs 4, 17, 18, the magnitude of η for viscous flow of crystalline bodies of constant chemical compostion is given by:

$$\frac{1}{\eta} = \frac{1}{L^3} \frac{D\Omega}{kT}. \qquad (13)$$

where D is the self-diffusion coefficient, Ω is the volume per atom, k is the Boltzman constant, T is the absolute temperature, and L some characteristic dimension, for example the mean diameter of the subgrains (mosaic blocks) free of dislocations (Ref 17), or the mean dimension of the grains (Ref 18).

Assuming that for the case of sufficiently small grains (to about 10 microns) L is determined by the dimension of the grains, then a change in viscosity may be noted as the mean dimension of the grains (particles) changes with their growth. Since the growth of the grains during secondary recrystallization takes place in accordance with the parabolic law (Ref 19):

$$l^2 = l_0^2 + K\sigma V t, \qquad (14)$$

where l is the mean dimension of the grains at time t, l_0 is the initial dimension of the grains, K is the reaction constant, σ is the surface tension at the grain boundary, and V is the volume of a gram-molecule. Then, substituting expression (14) in place of L^2 in equation (13), the change of viscosity with time may be given in the form

$$\frac{1}{\eta(t)} = \frac{D\Omega}{l_0^2 \left(1 + \frac{K\sigma V}{l_0^2} t\right) kT}. \qquad (15)$$

Denoting $b = \frac{K\sigma V}{l_0^2}$ and noting that $\frac{1}{\eta_0} = \frac{D\Omega}{l_0^2 kT}$, where η_0 is the viscosity at t = 0, corresponding to the dimension of the grains l_0, we arrive at the following variation of the shearing viscosity of the compacted material with time:

$$\eta(t) = \eta_0(1 + bt). \qquad (16)$$

Substituting this relation in the right part of equation (11) we obtain the variation of the change in porosity with pressure and duration of sintering:

$$F(f) = \frac{P}{4\eta_0 b} \ln(1 + bt), \qquad (17)$$

which is applicable for the described process of the compaction of powders of crystalline materials by hot pressing.

The value of the coefficient b which we introduced may be rather easily determined from the data of the metallographic determination of the mean dimension of the grains as a function of the duration of sintering from the formula

$$b = \frac{l^2 - l_0^2}{l_0^2 t}. \qquad (18)$$

In the case where the characteristic dimension L is determined from the dimension of the subgrains, the value of b will differ very little from that found by formula (18), since the growth of the grains takes place by the same diffusion mechanism and, in addition, b represents the relative squared rate of growth of the grains which should not change for a proportional reduction of the value of l entering in it. The existence of porosity and incomplete contact between particles may influence the magnitude of b.

However, for sintering temperatures amounting to 3/4 or more of the melting temperature, the retarding influence of porosity, as shown in experiments (Ref 18) is not noted.

It should be noted that a relation of the type of equation (16) has been derived by another method for the change in the rate of the non-steady creep for any (large or small) tension in Ref 30.

We used equation 17 for analyzing experimental data on the sintering by hot pressing of WC powder. The sintering of tungsten carbide, of composition close to stoichiometric and having mean grain dimensions as determined by microscopic investigation of the powder of about 1C

microns, was conducted in graphite moulds at temperature intervals of 100° from 2000 to 2700° under pressures of 70-165 kg/cm². The change in porosity and density of the samples was determined by the dilatometric method with continuous observation of the shrinking process. From the results of the shrinkage measurements the magnitude of the previously determined deformation of the loaded graphite components of the mould were subtracted. After sintering and careful cleaning of the adhered graphite the samples were measured and weighed. The density of the samples was determined by the method of hydrostatic weighing.

Since the law of constant mass is valid in sintering by hot pressing and constant cross section of the sample is maintained, the instantaneous density of the samples ρ' is found from the measured values of the final density ρ'', the final height h'' and the instantaneous measured height h' of the sample from the relation

$$\rho' = \frac{\rho'' h''}{h'}$$

where h' differs from h'' by the magnitude of the absolute shrinkage Δh.

From the calculated values of the density, the porosity of the samples was found

$$f = 1 - \frac{\rho'}{\rho_k} = 1 - p,$$

where ρ' is the density of the sample, ρ_k is the density of the compacted material, and p is the relative density.

Fig 2 shows the variation of the relative density of the samples as a function of the duration of the sintering and Fig 3 the variation of F(f) with ln(1+bt) as determined from formula (10). The value of the coefficient b determined from the results of the metallographic investigation of the hot pressed samples is shown in Table 1.

As can be seen from these data, F(f) varies linearly with ln(1+bt) which indicates the agreement of equation (18) with the experimental data. The value of the coefficient of shearing viscosity of the compacted material may be easily found graphically from the slope of the lines in Fig 3. To obtain more precise values we calculated values of η_0 by the formula resulting from equation (17):

$$\eta_0 = \frac{P \cdot \lg(1+bt)}{8 \cdot 0{,}4343 \cdot b \cdot F(f)},$$

where the coefficient 6 rather than 4 appears in the denominator to account for the non-uniform compression where $P_{(mean)} = \frac{1}{3}(P_1 + P_2 + P_3) = \frac{2}{3}P$ (P_1, P_2, P_3 are the normal applied stresses and P is the pressing pressure).

Table 1

Values of coefficient b, viscosity η_0 and energy of "loosening"

Температура, °С	Давление, кг/см²					
	70		130		165	
	b, 1/мин	η_0, г/см·сек	b, 1/мин	η_0, г/см·сек	b, 1/мин	η_0, г/см·сек
2100	0,015	$2,60 \cdot 10^{11}$	0,025	$2,94 \cdot 10^{11}$	0,035	$2,98 \cdot 10^{11}$
2200	0,022	$2,12 \cdot 10^{11}$	0,040	$1,72 \cdot 10^{11}$	0,045	$1,61 \cdot 10^{11}$
2300	0,030	$1,16 \cdot 10^{11}$	0,055	$8,90 \cdot 10^{10}$	0,070	$9,20 \cdot 10^{10}$
2400	0,045	$5,12 \cdot 10^{10}$	0,075	$5,70 \cdot 10^{10}$	0,090	$5,32 \cdot 10^{10}$
2500	0,055	$3,18 \cdot 10^{10}$	0,095	$3,70 \cdot 10^{10}$	0,110	$3,02 \cdot 10^{10}$
U, ккал/моль	84 500		77 000		78 000	

(a) Temperature, °C
(b) Pressure, kg/cm²
(c) b, 1/min
(d) g/cm-sec
(e) cal/mol

The calculated mean values of η_0 for tungsten carbide as a function of temperature and pressure are given in Table 1 while the variation of the viscosity of the compacted tungsten carbide with duration of sintering at a constant pressure of 165 kg/cm² as calculated from equation (17) is given in Fig 4.

The data of Table 1 show that the viscosity η_0 determined at t = 0 decreased with temperature. The variation of the viscosity with temperature, according to equation (13), may be presented in the form

$$\frac{1}{\eta} = \frac{\text{const}}{T} e^{-\frac{V}{RT}}, \qquad (19)$$

where U is the energy of "loosening" of the lattice of the compacted material, and R is the gas constant.

Thus, by means of simple transformations we may obtain the theoretical formula for finding the energy of activation of "loosening" of the lattice:

$$U = \frac{RT_1T_2}{T_2 - T_1}\left(\ln\frac{T_2}{T_1} + \ln\frac{\eta_{01}}{\eta_{02}}\right), \qquad (20)$$

where η_{01} and η_{02} are the viscosities corresponding to the temperatures (on the absolute scale) T_1 and T_2. The mean values of the energy of "loosening" for the WC lattice calculated in accordance with this formula are shown in Table 1.

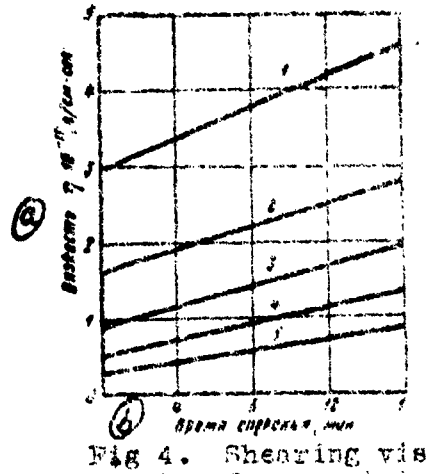

Fig 4. Shearing viscosity of compacted tungsten carbide vs sintering time for temperatures of: 1 - 2100, 2 - 2200, 3 - 2300, 4 - 2400, 5 - 2500°
ⓐ viscosity 10^{-11}, g/cm-sec
ⓑ sintering time, min

The energy of "loosening" for practical purposes does not vary with the applied pressure. This indicates that the process of deformation of the WC particles takes place by a diffusion mechanism in accordance with the viewpoint presented in this paper. In addition, this is in agreement with the statement in Ref 4 that in the case of 3-dimensional compression the increase in pressure will lead to the increase in the rate of diffusion creep without the occurrence of plastic deformation.

In a similar fashion we made a quantitative analysis of the experimental data of Hamjian and Lidman (Refs 21,22) on the hot-press sintering of chromium carbide, Cr_3C_2, at temperatures of 1370 - 1590° under a pressure of 140.6 kg/cm². Fig 5 shows the variation of F (f) with lg(1+ kt) for Cr_3C_2 and Table 2 lists the values of the coefficient b and the viscosity η_0 of chromium carbide. The change in viscosity during sintering determined from formula (16) is shown on Fig 6.

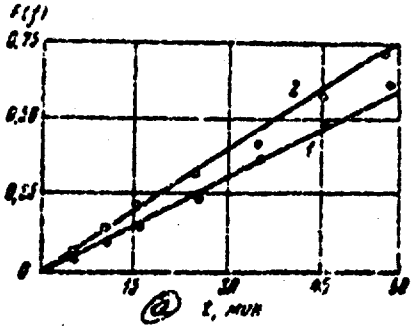

Fig 2. Reduced variation of porosity F(f) vs time of sintering for glass at pressures of:
1 - 40 kg/cm^2; 2-56 kg/cm^2
(a) t, min

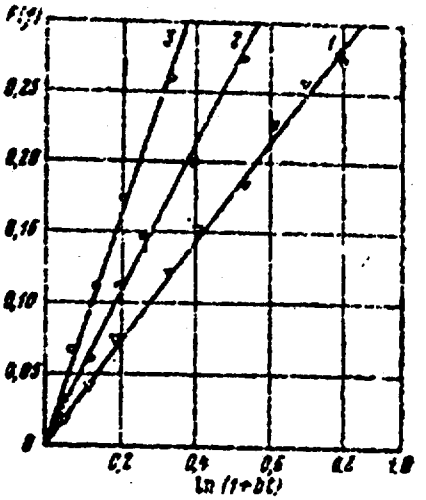

Fig 3. Reduced variation of porosity vs time of sintering of tungsten carbide at 2300° and pressures of:
1 - 70, 2 - 130, 3 - 165 kg/cm^2

Table 2

Values of the coefficient b, the viscosity η_o and the energy of "loosening" of the Greer lattice

(a) Temperature, °C	(b) b, 1/min	(c) η_o, g/cm-sec	Temperature, °C	b, 1/min	η_o, g/cm-sec
1470	0,015	$1,93 \cdot 10^{11}$	1540	0,020	$3,08 \cdot 10^{10}$
1480	0,018	$7,32 \cdot 10^{10}$	1590	0,032	$1,46 \cdot 10^{10}$

(a) Temperature, °C
(b) b, 1/min
(c) η_o, g/cm-sec

Note: U = 81,800 cal/mol

The theory presented here is in agreement with the qualitative observations of Hamjian and Lidman (Ref 21) which showed that the sintering process using hot pressing could be separated into three stages:
1) the formation of bonds between particles
2) increase in density with simultaneous increase in particle dimensions
3) growth of the grains without noticeable increase in sample density.

The derived equation (17) may be used as a basis for a rational selection of the sintering conditions in the hot pressing of powders.

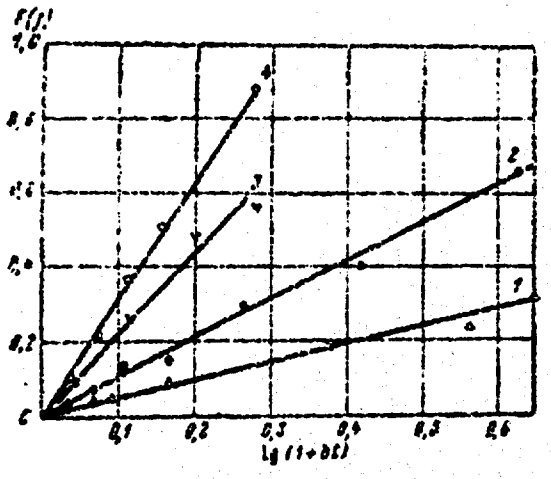

Fig 5. Reduced change in porosity F(f) vs time of sintering for chromium carbide under a pressure of 140.6 kg/cm^2 at temperatures of:
1 - 1370, 2 - 1480,
3 - 1540, 4 - 1590°

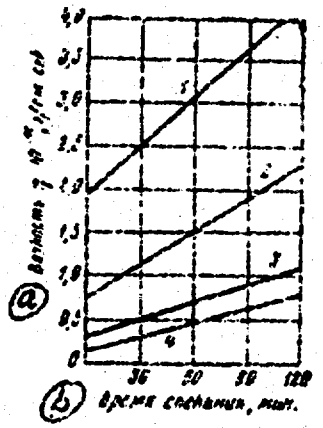

Fig 6. Shearing viscosity of compacted chromium carbide vs time of sintering at temperatures of:
1 - 1370, 2 - 1480,
3 - 1540, 4 - 1590°
ⓐ viscosity 10^{-11}, g/cm-sec
ⓑ sintering time, min

A simple calculation using equation (17) shows that for $\eta_0 = 10^{10}$ g/cm-sec and b = 0.03 min^{-1} the compaction (sintering) time from an initial porosity of 45% to a porosity of 1% under a pressure of 150 kg/cm^2 is about 7 minutes. For $\eta_0 = 19^{11}$ g/cm-sec and b = 0.01 min^{-1} the time is 1100 hours.

Thus, the process of sintering takes place relatively quickly when η_0 is about 10^{10} g/cm-sec. The refractory compounds under optimum conditions of sintering by hot pressing (Table 3) as established by experiment possess this order of coefficient of shearing viscosity.

In this work we have not considered the slippage along the boundaries of the grains which would be significant at the large values of the porosity which occur when incomplete packing of the particles is present. With increase in compaction this effect will diminish sharply.

As we have indicated earlier (Refs 2, 11) equation (1) can also satisfactorily describe the process of compaction of powders by hot pressing if consideration is taken of the variation of η with time. However the values of η_0 calculated using this formula from experimental data are approximately half of the correct values.

These considerations relate to the irreversible

Table 3

Conditions for sintering by hot pressing of powders of the refractory compounds

(a) Соединение	(b) Температура спекания, °С	(c) Давление на спекаемый порошок, кг/см²	(d) Время спекания, мин	(e) Остаточная пористость спеченного изделия, %
TiC	2700	120	2	0,5—3
ZrC	2700	120	5	2—3
NbC	3000	100	5	6—7
TaC	2600	120	5	5—6
Cr_3C_2	1750	120	5	0,7—1
Mo_2C	2400	120	5	9—10
WC	2000	100	5	1—2
TiN	2650	120	10	1—3
ZrN	2400	120	5	0
TaN	2230	120	5	0
TiB_2	2600	120	5	0,6—1
ZrB_2	2350	120	15	0
CrB_2	2100	120	5	0
NbB_2	2580	120	10	0
TaB_2	2350	120	10	8—9
Mo_2B_5	2000	120	5—7	0,5—1
W_2B_5	2200	120	5	0,6—1
CaB_6	2200	220	10	2—3
LaB_6	2.5-1	120	10	1
CeB_6	2150	120	5	2
YB_6	2150	120	5	0,8—1
$TiSi_2$	1400	250	7	0.2—2
$ZrSi_2$	1100	250	10	5—6
$NbSi_2$	1900	220	10	0
$TaSi_2$	2100	250	10	0
$MoSi_2$	1100	250	10	0
WSi_2	1950	250	5	0
$FeSi_2$	1170	250	10	7—8

(a) compound
(b) sintering temperature, °C
(c) sintering pressure, kg/cm²
(d) sintering time, min
(e) residual porosity of the sintered product, %

change in density of sintered bodies. At the same time, during hot pressing reversible changes of the density after removal of the external pressure are noted which are related with the relaxation of the volume. This effect may be significant for porous semi-crystalline bodies. The reversible change in density which we investigated in the

sintering of Mo_2C powder by hot pressing is satisfactorily described by the exponential equation:

$$\frac{\Delta\rho}{\rho_0} = \text{const.} e^{-\frac{t}{\tau}}$$

where $\Delta\rho/\rho_0$ is the relative reversible change in density, ρ_0 is the equilibrium density established after relaxation, and $\tau = \tau_0 e^{U/RT}$ is the relaxation time.

It was found that for Mo_2C over the temperature range of 2000-2300°C $\tau_0 = 6.90$ sec and $U = 75,000$ cal/Mol.

CONCLUSIONS

1. An analysis of the process of the compaction by sintering of porous powders was carried out and the variation of the rate of compaction when sintering powders by hot pressing as a function of the applied pressure was obtained.

2. When sintering the powders of crystalline materials it is found that there is a linear variation of the viscosity of the compacted material with sintering time.

3. An experimental verification of the derived relationships for the sintering of tungsten carbide powder by hot pressing was conducted and the values of the viscosity at sintering temperatures and the energy of loosening of the lattice of tungsten carbide were determined.

4. A quantitative analysis of the available literature data on the sintering by hot pressing of chromium carbide was made and the values of the viscosity of Cr_3C_2 at sintering temperatures and the magnitude of the energy of loosening of the lattice of Cr_3C_2 were determined.

5. The relationships derived may be used for the sintering of powders by hot pressing.

REFERENCES

1. M.S. Koval'chenko, G.V. Samsonov. USSR AS News, Division of Technical Sciences, Metallurgy and Fuel, No 4, 1959
2. G.V. Samsonov, M.S. Koval'chenko. Hot Pressing Ukrainian SSR State Technical Press, Kiev, 1962
3. Ya. I. Frenkel', ZhETF (Journal of Experimental and Theoretical Physics), 16, 1946
4. B.Ya. Pines. UFN (Progress in Physical Science), 52, 1954
5. C. Herring. Physics of Powder Metallurgy. 1951
6. J. Mackenzie, R. Shuttleworth. Proc. Phys. Soc., 62-B, 1949
7. Ya.E. Geguzin, B.Ya. Sukharevskiy, ZhTF (Journal of Theoretical Physics), 24, 1954
8. P. Murray, E. Rogers, A. Williams. Trans. Brit. Cer. Soc., 53, 1954
9. G. Mangsen, W. Lambertson, B. Best. J. Am. Cer. Soc., 43, 1960
10. T. Gray. The Defect Solid State, Interscience Publishers, 1957
11. G.V. Samsonov, M.S. Koval'chenko. Powder Metallurgy, 1, No 1, 1961
12. J. Mackenzie. Proc. Phys. Soc., 63-13, 2, 1950
13. L.D. Landau, E.M. Li[illegible]ts. The Mechanics of Continuous Media. State Technical and Theoretical Press, 1954
14. V.V. Skorokhod. Engineering Physics Journal, 3, No 11, 1960
15. G.I. Gurevich. "Certain Problems of the Mechanics of Deformable Media." Reports of the Institute of Earth Physics, No 2, USSR AS Press, 1959
16. J. Williams. Symposium on Powder Metallurgy, 1954. Iron and Steel Inst., London, 1956
17. F. Nabarro. "Report on a Conference of the Strength of Solids." Phys. Soc., London, 1948
18. C. Herring. J. Appl. Phys., 21, 1950
19. J. Burke, D. Turnbull. Progress in Physical Metallurgy, Vol 1, Metallurgical Press, 1956
20. L.M. Shestopalov. Deformation of Metals and Plastic Waves in Metals. USSR AS Press, 1958
21. H. Hemj'ian, W. Lidman. J. Metals, 5, 1953
22. H. Hausner. Symposium on Powder Metallurgy, 1954, Iron and Steel Inst., London, 1956

10484
CSO: 1879-S

- END -